New Silica-Immobilized Nickel Catalysts for Cyclotrimerizations of Acetylenes

S. Reinhard, P. Šoba, F. Rominger, J. Blümel*

Department of Organic Chemistry, University of Heidelberg, Im Neuenheimer Feld 270, 69120 Heidelberg, Germany
Phone: (+49)-6221-54-8470, Fax: (+49)-6221-54-4904, e-mail: J.Bluemel@urz.uni-heidelberg.de

Received: December 16, 2002; Accepted: February 6, 2003

Abstract: New dicarbonylnickel catalysts with a variety of mono- and bidentate phosphine ligands, such as $Ph_2P(CH_2)_xPPh(CH_2)_ySi(OEt)_3$ ($x = 2, 3$; $y = 2, 3$), have been synthesized and fully characterized, three of them by X-ray analyses. All the catalysts have been immobilized on silica by reaction of the ethoxysilane or hydroxy groups of the phosphine linkers with the surface silanol groups. The clean immobilization was proved by ^{31}P solid-state NMR. It has been demonstrated that the C–O–Si bridge, in contrast to the strong Si–O–Si bond, is easily cleaved by organic solvents and water. With respect to the cyclotrimerization of phenylacetylene the optimal reaction conditions for all molecular and immobilized catalysts have been determined. Cyclooctane was the best solvent, and the optimal reaction temperature was 100 °C for reactions in homogeneous phase, and 155 °C for surface-bound catalysts. The bite angles and spacer lengths of the chelating ligands did not play a major role for the performance of the homogeneous or immobilized catalysts. The latter could be recycled for 12 times, with final substrate conversions still typically between 30 and 40%, and turnover numbers (TON) around 1500. With an excess of substrate in one run a TON of 4810 was obtained for an immobilized carbonylnickel complex with a dppp-type chelate phosphine ($x = 3$, $y = 2$). Reduction of the surface coverage generally resulted in catalysts with longer lifetimes, for example, reduction to one fourth gave a record TON of 7616 for this catalyst. The selectivities of the catalysts all followed one trend. The main products were the cyclotrimers 1,2,4- and 1,3,5-triphenylbenzene, besides dimers, linear trimers and tetramers as side-products. The fraction of the latter decreased at higher temperatures with homogeneous catalysts, and vanished entirely after a few cycles with the immobilized catalysts. On recycling, the initial ratio of unsymmetrical to symmetrical cyclotrimers of typically 5:1 gradually changed to about 1:1 for all catalysts.

Keywords: alkynes; cyclotrimerization; immobilization; nickel catalysts; P ligands; silica; solid-state NMR

Introduction

Catalysis represents one of the most central aspects of chemistry, and the quest for “ideal catalysts”[1] is being pursued in many laboratories world-wide. Many types of approaches are being undertaken. For example, homogeneous catalysts are made more and more efficient by tailoring,[2] or two different catalysts are combined.[3] Alternative recent strategies for improved removal of the catalysts from the reaction mixtures make use of biphasic fluorous systems,[4] microencapsulation of catalysts,[5] or non-covalently functionalized dendrimers.[6] The key feature of all these different approaches is to improve catalyst recovery and recycling.

For some time our group, like others,[7,8] has pursued this idea by immobilizing homogeneous catalysts on oxidic inorganic supports.[9–14] Since the tethering is achieved by bifunctional linkers such as $Ph_2P(CH_2)_3Si(OEt)_3$ (**1**),[9] the homogeneous character of the catalysts should be retained, while the solid support allows the easy separation of the catalyst by decanting the supernatant reaction mixture. Thus, ideally, the advantages of homogeneous and heterogeneous catalysts should be combined. However, the major drawback of immobilized catalysts is their possible detachment from the support, the leaching. In the course of our studies, we examined a variety of possible leaching mechanisms, and could successfully eliminate them by simple means. For example, the support material best suited for the irreversible reaction with ethoxysilane groups is silica, while oxides like MgO, TiO_2 or acidic Al_2O_3 lead to extensive and permanent linker leaching.[15] With silica, the different forms of leaching can be prevented efficiently by applying the right conditions concerning solvent[16] and temperature[17] during the immobilization step, and using rigorously dried silica.[16,18] As soon as there is one covalent Si-O-Si bond established, the linker is irreversibly bound.[15] Detachment of the metal fragment from the phosphine moieties[11,12] can be prevented by chelat-

DOI: 10.1002/adsc.200202206

ing phosphines with ethoxysilane groups.[10,12,14] As we have demonstrated recently, catalyst deactivation by dimerization can also be inhibited by diluting the metal centers on the surface.[12,14]

The surface-modified supports are amorphous materials, and thus cannot be characterized with conventional analytical methods other than IR. Nowadays, the method of choice to study the immobilized species is classical solid-state NMR, which we have optimized especially for the measurement of immobilized phosphines and molecular catalysts.[19] As a complementary method, suspension NMR spectroscopy[15,20] allows the rapid check of a great number of routine samples, and also helps to detect merely adsorbed in contrast to covalently bound species.[15,18]

The cyclotrimerization of alkynes represents one of the most useful methods for the selective synthesis of various substituted aromatic compounds.[21] Since many transition metal complexes are active catalysts for cyclotrimerizations, it is not surprising that the interest in both mechanistic as well as synthetic aspects of cyclotrimerizations has even been growing recently. Regarding the mechanism of cyclotrimerizations, it is nowadays generally agreed that a metallacyclopentadiene is involved. This is corroborated by theoretical studies,[22,23] as well as by experimental evidence. Using unreactive alkynes or bulky phosphine ligands, many trigonal planar bisphosphinemonoalkyne complexes could be isolated by Pörschke,[24] for example, $(Cy_3P)_2Ni(\eta^2\text{-}C_2H_2)$,[24] and by others, e.g., $(Ph_3P)_2Pd(\eta^2\text{-}MeO_2CC{\equiv}CCO_2Me)$,[25] $[\eta^2\text{-}i\text{-}Pr_2PCH_2CH_2P\text{-}i\text{-}Pr_2]Ni(\eta^2\text{-}PhC{\equiv}CPh)$,[26] $(\eta^2\text{-}Cy_2PCH_2CH_2PCy_2)Ni(\eta^2\text{-}PhC{\equiv}CPPh_2)$.[27] There are also recent preparative mechanistic studies discussing metallacyclopentadienes, e.g., with Fe as the metal center,[28] Ni,[29–31] Ti,[32,33] Zr,[34] Rh,[35–37] Ru,[38,39] lanthanides,[40] and actinides.[41] Although different types of model compounds have been synthesized,[42–44] the final step is still a matter of debate. Out of the many recent applications of cyclotrimerizations for directed syntheses of aromatic systems,[28–41,45–49] perhaps the most spectacular are the syntheses of helicenes,[50] and of dendrimers.[51]

Our goal has been now to further improve catalytic cyclotrimerizations by applying immobilized catalysts, and thus make these reactions more efficient. Out of the many possible metals we have chosen Ni(0) catalysts. Carbonylnickel complexes in particular have the advantage that they are cheap, easily prepared, and good for analytical purposes, because they are not paramagnetic, which can, e.g., be demonstrated by their ^{61}Ni NMR data.[52] The carbonylnickel complexes are well-defined, and they need no cocatalyst for the cyclotrimerizations. Although they are known to oligomerize or polymerize a variety of different acetylenes, depending on the reaction conditions,[53] for our detailed and systematic study phenylacetylene as the substrate is suited best. The cyclotrimerization of phenylacetylene gives two isomers, the unsymmetrical 1,2,4- and symmetrical 1,3,5-triphenylbenzene, besides a minor amount of linear dimers and trimers. The product mixture can easily be analyzed by GC, and in this way the activity and selectivity of the catalyst can be checked simultaneously in one catalytic run. The starting material phenylacetylene is volatile and can easily be removed under vacuum from the reaction mixture if necessary.

Here, we present a systematic study of a variety of carbonylnickel catalysts in the homogeneous phase, as well as immobilized on silica. We will examine the effect of the reaction conditions, of the binding to the support, and factors like bite angle and spacer length of different ligands. It will be shown that very efficient recyclable catalysts can be obtained by quite simple measures.

Results and Discussion

Synthesis of the Phosphine Ligands

All the phosphine ligands relevant for this work are displayed in Scheme 1. The ligands **1** to **3** have been synthesized in high yields as described previously,[9,17] as well as the phosphines **4**–**9** in yields of 89–93%.[10] They have been fully characterized by the usual analytical methods, and the NMR signal assignments are based upon former results,[9,10,13,17] and $^{13}C\{^{31}P\}$, H,H-, H,C-, H,P-COSY, and H,P-HOESY spectra. The still unpublished data of the compounds **7** – **9** are given in the Experimental Section. In solution all the phosphines are air-sensitive, and even the most robust triarylphosphine **2** should be handled under nitrogen or argon in Schlenk flasks or in a glove-box carefully. However, as soon as the phosphines are immobilized on silica, they can be fully exposed to the air for hours, until measurable amounts of phosphine oxide appear in the ^{31}P NMR spectra.[19] The methods of choice for purifying the phosphines is Kugelrohr distillation or reversed phase chromatography.

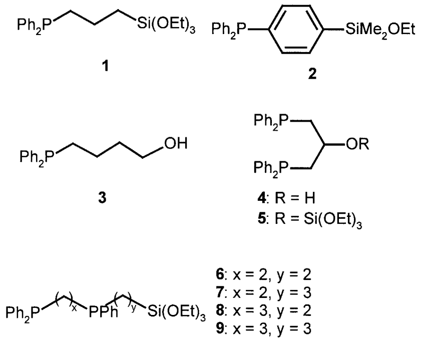

Scheme 1. A variety of monodentate and chelating phosphine linkers **1** – **9**.

Synthesis of the Nickel Catalysts

The most relevant nickel catalysts investigated in this work are displayed in Scheme 2. Only the complexes **10**,[9] **12**,[9] and **16**[10] have been described previously. Data for the new systems are given in the Experimental Section. Due to the alkyl chains and ethoxysilane groups, all the compounds are viscous oils, which can only be crystallized occasionally (see below).

Nevertheless, preparing the molecular catalysts prior to immobilization has two advantages. First, the complexes can be prepared with the correct stoichiometry and purified. This leads to cleaner immobilization than with catalysts prepared on silica. Furthermore their analytical data, for example even $\delta(^{61}Ni)$ and $^{1}J(^{61}Ni\text{-}^{31}P)$ values can be obtained.[52] In order to avoid the toxic $Ni(CO)_4$ for the preparation of the carbonylnickel compounds,[52] we apply two routes (Scheme 3). In the first route $(COD)_2Ni$ is treated with the phosphine, e.g., **7**, and **20** forms, as one COD ligand is replaced. The second coordinated COD is then replaced by CO to form **17** by bubbling carbon monoxide into the reaction mixture.[10,54] This route can be pursued under very mild conditions in organic solvents, and is therefore also suitable for phosphines containing an ethoxysilane group that might lead to side reactions[17] or cross-linking[16] otherwise. For phosphines with OH instead of SiOEt groups, such as **3** and **4**, route 2 can be applied. Here, for example in the case of **3**, starting from $NiCl_2 \cdot 6\,H_2O$ the dichloronickel complex **21** can be formed first, and then reduced with Zn under addition of CO to the corresponding carbonylnickel complex **11**.[55] Using the sulfur compound $NaSCH_3$ as an alternative to Zn[56] is possible, but less pleasant and practicable.

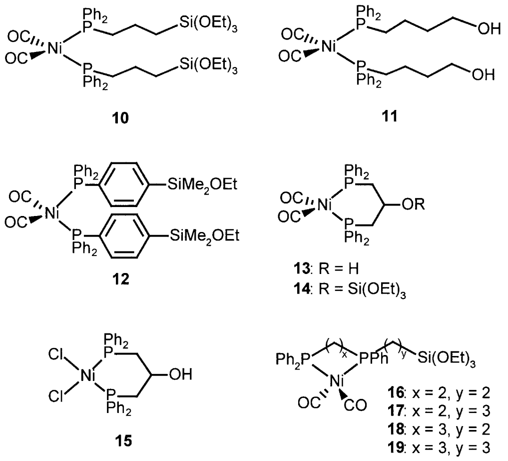

Scheme 2. Molecular nickel catalysts with monodentate and chelating phosphine ligands.

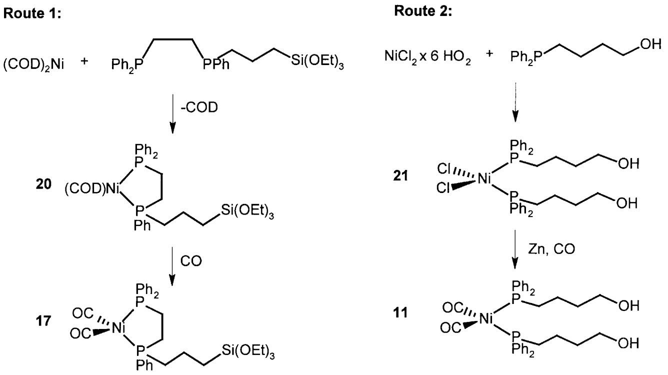

Scheme 3. Two possible routes for the synthesis of carbonylnickel phosphine complexes.

Characteristics of the Nickel Catalysts

NMR Properties of the Nickel Complexes

Interestingly, complex **21** in C_6D_6 at ambient temperature gave broad paramagnetic ^{1}H NMR signals[57] at 27 ppm (halfwidth about 1.5 kHz) and 9 ppm, besides broad signals in the diamagnetic region. More detailed studies and signal assignments will be a subject of future investigations. However, this result is in accord, for example, with the finding of Fyfe's group[58] for the analogous complex $[(EtO)_3SiCH_2CH_2PPh_2]_2NiCl_2$, which was reported not to give a ^{31}P NMR signal at room temperature. Obviously, these complexes are tetrahedral, although some other dichloronickel complexes with diarylalkylphosphine ligands that we and others have investigated so far,[19,59] including **15** (see below) are planar and diamagnetic, and they give ^{31}P and ^{13}C CP/MAS signals with small halfwidths.[19,59] A more detailed overview of diamagnetic *versus* paramagnetic Ni(II) diphosphine complexes has been given by Booth.[60]

All the other diamagnetic nickel complexes have been fully characterized by the usual analytical methods, and the NMR signal assignments are based upon former results,[9,10,13,17] comparisons with values from the literature[61] and $^{13}C\{^{31}P\}$, H,H-, H,C-, H,P-COSY, and H,P-HOESY spectra. The obtained nickel complexes can also nicely be measured as polycrystalline materials by ^{31}P- and ^{13}C CP/MAS NMR, and we even used them as standard samples for recording the solid-state NMR spectra for all sorts of similar immobilized species.[19] The linewidths of these polycrystalline samples are rather small, with about 100 to 150 Hz, depending on the method of measurement. All polycrystalline dicarbonyl- and dichloronickel complexes with chelating phosphines show two well-resolved and narrow ^{31}P NMR resonances[19] in the solid state, indicative of two magnetically non-equivalent phosphorus nuclei in the elemental cell.

Crystal Structures of the Nickel Complexes

The square planar arrangement of the ligands at the metal center of **15** (Figure 1) can be demonstrated by an

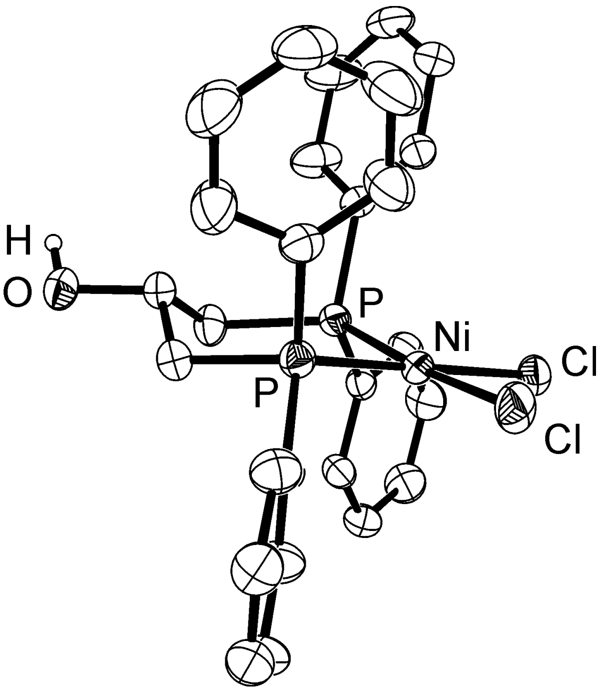

Figure 1. Molecular structure of **15**. Anisotropic replacement parameters are shown at 50% probability level, hydrogen atoms except O<u>H</u> have been omitted for clarity. Details of measurement see ref.[62] Selected angles [°] and bond lengths [Å]: P–Ni–P 94.08(2); Cl–Ni–Cl 91.94(1); P–Ni–Cl$_{cis}$ 86.47(2)/87.43(2); P–Ni–Cl$_{trans}$ 174.96(2)/178.26(3); Ni–Cl 2.2191(6)/2.2089(6); Ni–P 2.1652(6)/2.1800(6).

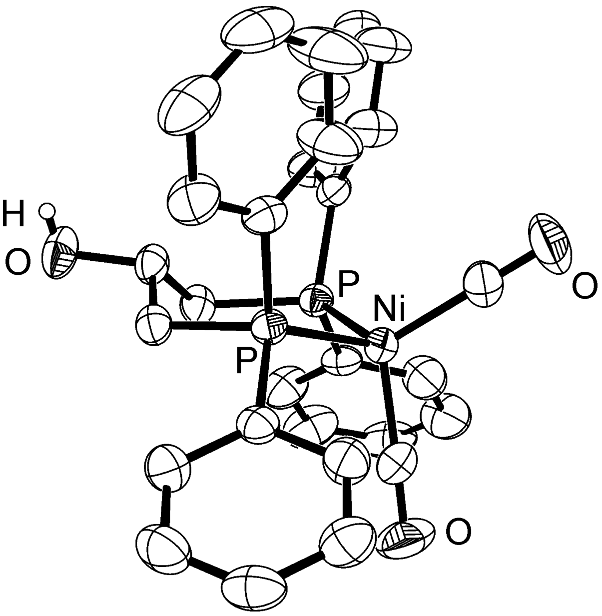

Figure 2. Molecular structure of **13**. Anisotropic replacement parameters are shown at 50% probability level, hydrogen atoms except O<u>H</u> have been omitted for clarity. Details of measurement see ref.[64] Selected angles [°] and bond lengths [Å]: P–Ni–P 101.35(2); C–Ni–C 114.46(10); P–Ni–C 107.20(7)/105.82(7)/114.24(7)/114.46(10); Ni–C 1.768(2)/1.774(2); Ni–P 2.1888(6)/2.1953(6).

X-ray analysis.[62] The arrangement of the molecules in the elemental cell corroborates the magnetic inequivalence of the two phosphorus nuclei found earlier in the form of two ^{31}P CP/MAS signals.[19] Due to the chelate ring the phosphine ligands have to assume a *cis* position in contrast to many complexes with monodentate phosphines, which prefer a *trans* arrangement and therefore display no dipolar moment.[60] The P–Ni–P angle is 94.08°, and thus in the usual range for this type of complex; for example, the P–Ni–P angle in the comparable compound $[(MeOCH_2)MeC(CH_2PPh_2)_2]NiCl_2$ is 95.49°.[63]

In contrast to the dichloronickel compounds the dicarbonylnickel complexes are all diamagnetic and thus tetrahedral. This can, for example, be seen in Figure 2, which shows the crystal structure of **13**.[64] The bite angle of the chelating phosphine P–Ni–P is widened to 101.34° now to accommodate the tetrahedral arrangement of the substituents. However, a comparison with the crystal structure of **11**[65] (Figure 3) with a P–Ni–P angle of 108.7° for analogous alkyldiaryl, but monodentate phosphine ligands, which comes close to the theoretical tetrahedral angle, shows that the chelate phosphine still imposes its steric requirements to the complex. This might have an impact on the catalytic activity of the nickel complexes (see below). Interestingly, on going from the dichloronickel complex **15** to the carbonylnickel complex **13** the two phenyl rings of the lower half of the molecule, which in **15** lie approximately in one plane with the P atoms perpendicular to the plane Cl–Ni–Cl, have to rotate about 90° in order to accommodate the steric needs of the CO ligand in **13**. In contrast to the complexes **13** and **15** with their bulky chelate ligands, intermolecular hydrogen bridges form in **11** (Figure 3, right display). Within the symmetrical assembly of the four OH groups, the distances between the O atoms are 2.75 and 2.80 Å, the two angles O–H ··· O are 173 and 178°. Since every complex has two phosphine ligands, in the solid state an extended network forms due to hydrogen bonding. This might have implications on the immobilization of phosphine **3** and its complexes on silica (see below). The crystal structure of **11** furthermore shows that there is no interaction of the oxygen atoms with the metal center, as it is claimed e. g. for Ru complexes with ether-containing phosphine ligands.[68]

Immobilization of the Linkers and Catalysts

Immobilized species will be denoted by **i** in the following. All the linkers and catalysts can be tethered to silica (Merck silica, specific surface area 750 m^2/g, average pore diameter 40 Å) as described previously.[1–3,9–13] Special care has to be taken regarding the tempera-

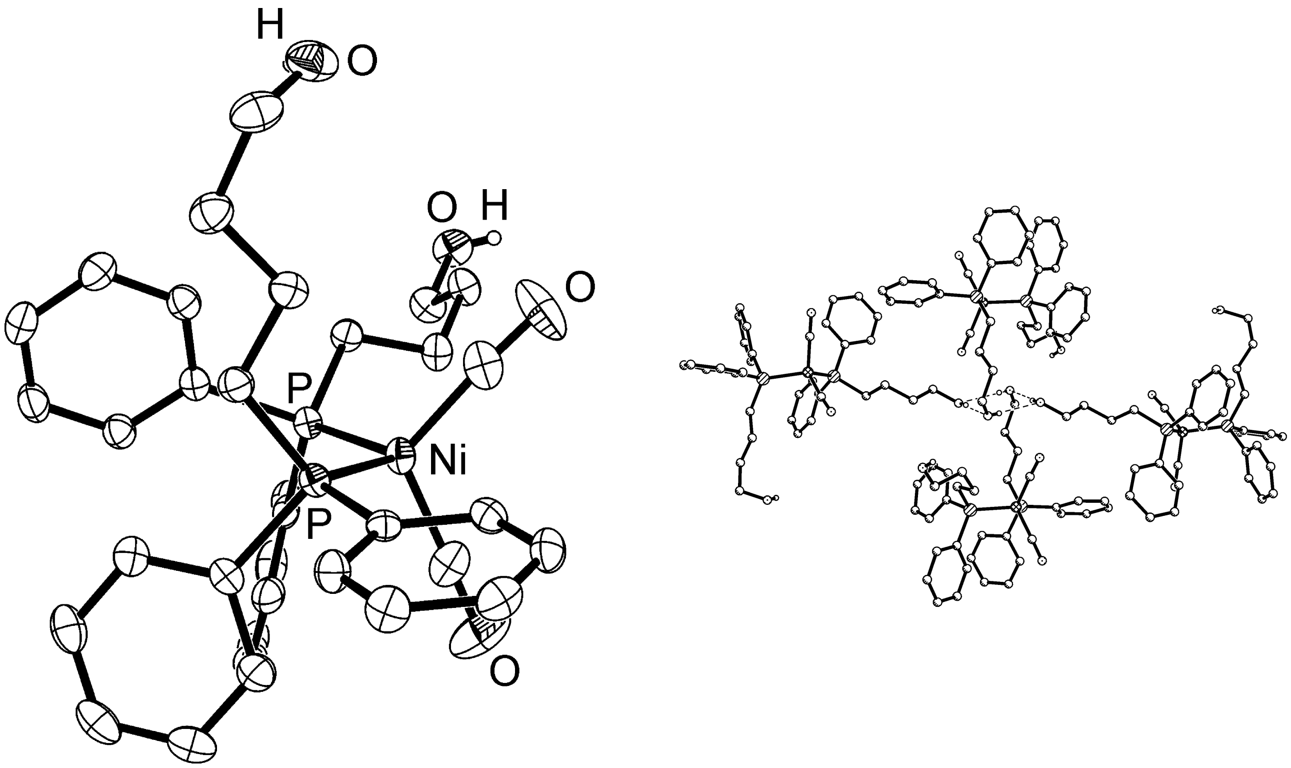

Figure 3. Molecular structure (left display) and an arrangement of four molecules (right display) of **11**. Anisotropic replacement parameters are shown at 50% probability level, hydrogen atoms except O<u>H</u> have been omitted for clarity. Details of measurement see ref.[65] P–Ni–P 108.67(2); C–Ni–C 113.50(12); P–Ni–C 104.88(8)/107.20(8)/107.99(8)/114.30(8); Ni–C 1.772(3)/1.775(3); Ni–P 2.2193(6)/2.2206(6).

ture[17] and the solvent[16] used for the immobilization. It is important that the temperature of the immobilization be as low as possible,[17] the silica be as dry,[18] and the solvent be as unpolar[16] as possible. In the case of immobilization *via* Si(OEt)$_3$ groups, as soon as one covalent bond is formed, the linker cannot be detached from the surface any more.[11,15] The success of the procedure can be checked with ^{31}P CP/MAS NMR,[19] as displayed in Figure 4 for the surface-bound ligand **6i** and complex **14i**.

Due to the inhomogeneity of the surface, the linewidths are increased by immobilization, e.g., to 775 Hz for **14i**. In the case of **6i**, the signals for both phosphorus nuclei, which have different chemical shifts in solution,[10] now overlap. However, the spectra show that ligands and complexes can be immobilized without any side-products.[17] Importantly, in the case of the nickel compound, no uncomplexed phosphine can be detected on the surface.[12]

Recently the formation of EtOH layers on silica surfaces in cyclohexane has been investigated.[69] The reaction of alcohols with silica has already been described by Iler[70] and one of us.[18] However, regarding the robustness of covalent bonding to the support in the case of ligands with OH groups, such as **3** and **4**, no systematic studies have been done yet to the best of our knowledge. Therefore, we undertook surface detachment studies, as we have previously done with ethoxysilane species.[15] The surface-modified silica was stirred with the solvents or mixtures as given in Table 1 for 24 h at ambient temperature. Then, the amount of ligand found in the supernatant solution was determined. In case a TLC analysis did not indicate the presence of any

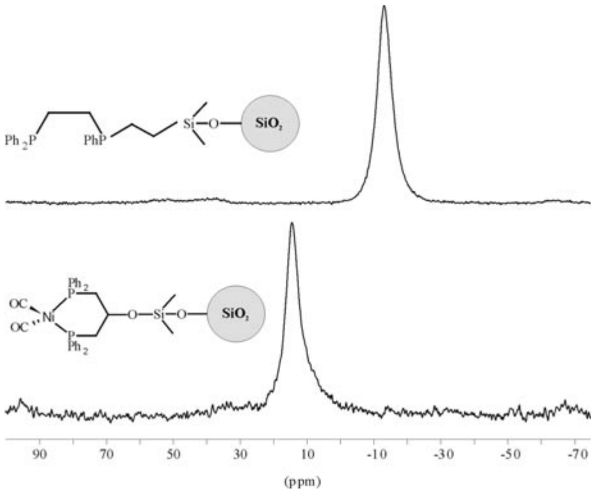

Figure 4. 162.0 MHz ^{31}P CP/MAS spectra of **6i** and **14i** on silica. Rotational frequency 13 kHz, other details of the measurement see ref.[19]

Table 1. Detachment experiments for **3i** and **4i** on 1 g of SiO_2 with 20 ml of solvent at ambient temperature.

Solvent	Ligand on SiO_2	Immobilized substance [mg]	Detached ligand [mg]	[%]
toluene[b]	**3**	63	–	–
toluene[b]	**4**	72	–	–
THF	**3**	78	< 5	< 6
THF[b]	**4**	82	6[b]	< 10[b]
ethanol	**3**	103	52	50
ethanol	**4**	75	64	85
ethanol[a]	**3**	70	70	100
ethanol[a]	**4**	45	42	94
ethyl acetate[a]	**3**	86	86	100
ethyl acetate[a]	**4**	78	63	85
acetone[a]	**3**	254	136	53

[a] Oxygen-free solvents with residual water content.
[b] 60 °C.

ligand in solution, 12 more h of stirring at 60 °C followed. As the examples in Table 1 show, with toluene **4** cannot be removed from the silica even at higher temperatures. However, more polar solvents lead to nearly quantitative loss of **4** from the surface already at room temperature. Especially the solvents with residual water content lead to major ligand leaching. This has to be taken into account in case leaching of the catalyst and/or linker is found later during recycling experiments. As compared to **4i**, **3i** is even more vulnerable to leaching. The reason might be the tendency to form intermolecular hydrogen bridges, as they were found for **11** in the crystal structure (see above). This tendency of **11** to arrange itself in extended networks leaves less opportunities for bonding to the silica surface *via* C–O–Si bridges. Thus, larger aggregates of **3** might assemble in the pores, which are later just flushed out by the solvent. The higher initial loading of silica with **3** as compared to **4** (Table 1) could also be explained with this sort of cross-linking *via* hydrogen bonds. Since for the recycling of catalysts a strong irreversible covalent bonding to the support is indispensable, and the catalysts **11i** and **13i** indeed showed too much leaching in repeated runs, in the following we will focus on the catalysts immobilized *via* siloxane bridges.

Cyclotrimerization of Phenylacetylene

Improvement of Catalysis Conditions in Homogeneous and Heterogeneous Phase

All the experiments described in this manuscript were done in a batch-wise manner, with a catalyst to substrate ratio of 1:200, and a phenylacetylene (**22**) concentration of 0.5 mol/L. The amount of catalyst applied here is rather small with 0.5 mol %, as compared to the 2–4 mol % used previously.[e.g.,46] As a first step we checked the influence of the solvent on the performance of the catalyst, and found that unpolar aliphatic hydrocarbons function best.[12] But even within this group there are marked differences. While, for example, catalyst **10** gives quantitative conversion of the substrate after 3 h at 100 °C in cyclooctane, under otherwise the same reaction conditions in decane even after 3 days the conversion is lower than 10%. This effect cannot be due to different polarities, because the dielectric constants of cyclooctane (2.12) and decane (1.99) are very similar.[71] Interestingly, there is even a noticeable difference between octane and cyclooctane (Figure 5). While the conversion/time curve has the same character, in octane only about 90% conversion can be obtained with **10**. This effect of the cyclic hydrocarbons, that we find for all the molecular and immobilized catalysts in this paper, is known since a long time among chemists working in the field of catalysis, but it has to the best of our knowledge never been explained. For the rest of the work presented here, cyclooctane was used as the solvent.

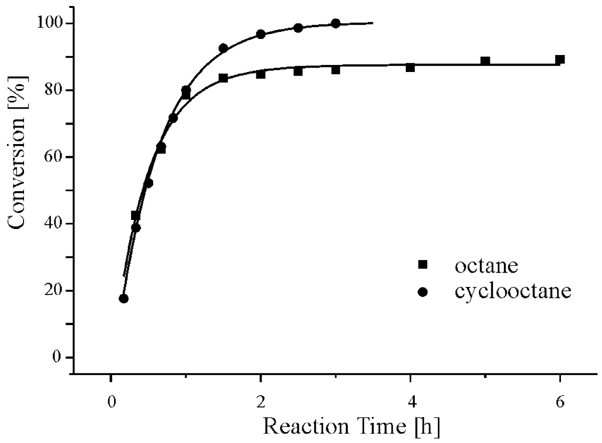

Figure 5. Representative dependence of the catalytic activity on the solvent for catalyst **10** with phenylacetylene (**22**).

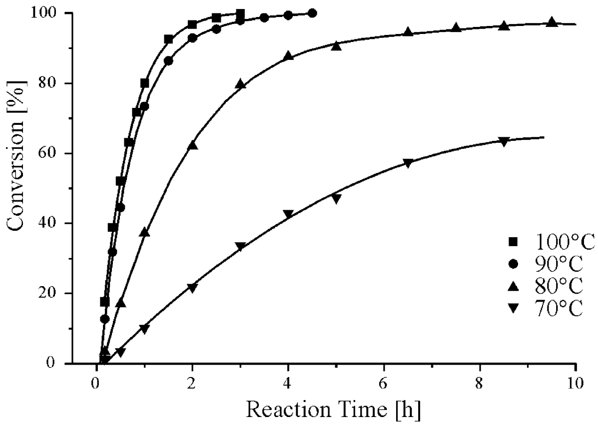

Figure 6. Temperature dependence of the catalytic activity of **10** in cyclooctane.

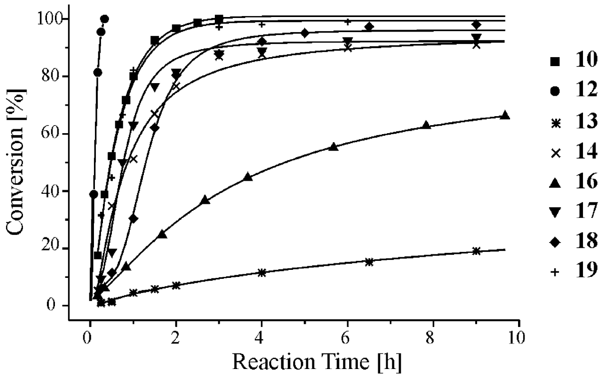

Figure 7. Comparison of the activities of **10**, **12** – **14**, and **16** – **19** in the homogeneous phase at 100 °C.

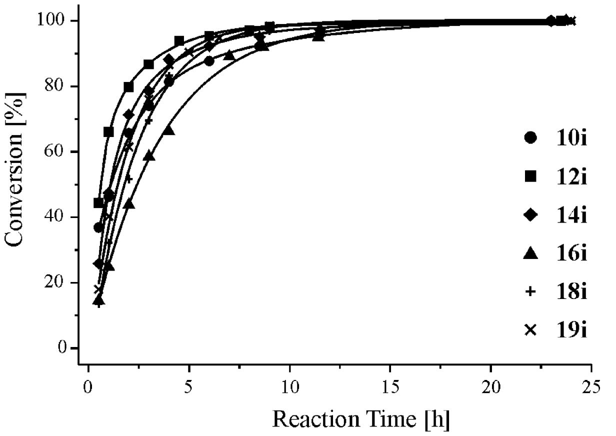

Figure 8. Comparison of the catalytic activities of **10i**, **12i**, **14i**, **16i**, **18i**, and **19i** at 155 °C. For **17i** see ref.[12]

Another positive effect of cyclooctane versus octane (bp 126 °C) is the higher boiling point of 152 °C, which allows catalytic runs with a bath temperature of up to 155 °C. With respect to the optimal temperature, all the homogeneous catalysts **10** – **19** have the same preferences as their immobilized analogues **10i** – **19i**. For catalysts with monodentate alkyldiarylphosphine and triarylphosphine ligands, 100 °C is a good choice. This is displayed for example in Figure 6 for **10**.

Triarylphosphine ligands lead to more active catalysts, for example, quantitative conversion of **22** is reached with **12** after about half an hour at 100 °C already, while about 3 hours are needed by **10** (Figure 6). All catalysts with chelating ligands need 155 °C for optimal activity. For example, at 155 °C with **19** quantitative conversion is achieved after less than half an hour, while 6 hours are needed at 100 °C. As another example, for **17** the relation is 3 h at 155 °C versus 9 h at 100 °C.

Comparison of Catalysts with Different Types of Ligands

Although 100 °C is not the optimal temperature for complexes with chelating ligands (see above), we chose it as a compromise in order to compare the activities of all the homogeneous catalysts **10** – **19**. The result is displayed in Figure 7.

Under these conditions, the most active catalyst is **12**, while **13** displays the worst performance, which might be due to its reduced solubility in cyclooctane. Otherwise, with the exception of **16**, all the complexes display similar activity. Complex **16** performs equally well at higher temperatures, though. Overall, one has to conclude that the bite angles or the spacer lengths of the chelating ligands do not have a decisive influence on the catalytic activity of **14** and **16** – **19**. Possibly the ligands are not rigid enough to show any obvious dependence of the catalytic performance on the bite angle.[72]

The previous results also showed that the cyclotrimerization is not sensitive towards minor changes of the linkers. Therefore, one could anticipate that the immobilized versions of the catalysts, **10i**, **12i**, **14i**, **16i**, **17i**, and **19i** are equally suited for cyclotrimerizing **22**. Indeed, as displayed in Figure 8, again all catalysts have similar activity and achieve 100% conversion within one day. The catalytic reaction is slower than in the homogeneous phase, because now the substrate has to diffuse into the pores of the support. This has been proved recently with Rh catalysts by using supports with different pore sizes.[14] However, this drawback is made up for by the easy separation of the catalyst from the reaction mixture by simply decanting the supernatant solution after the

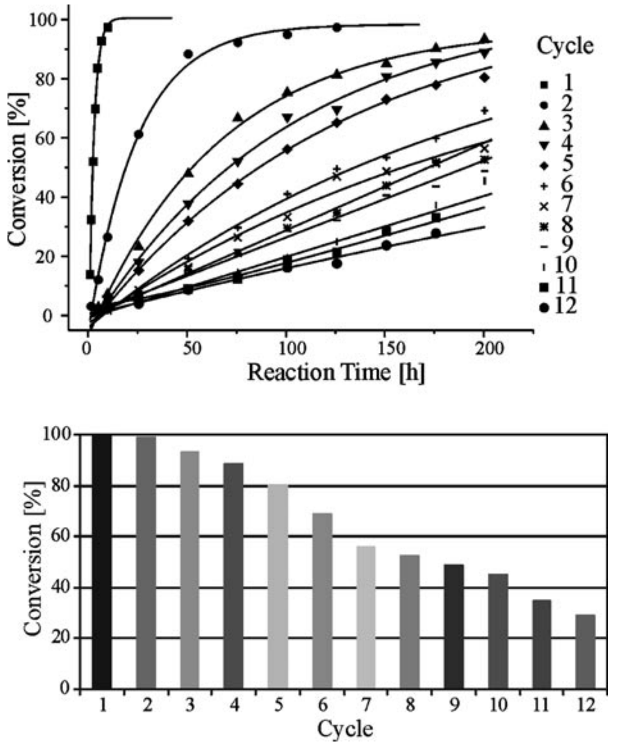

Figure 9. Recycling of **18i** in the cyclotrimerization of **22**. Top: Catalytic activities; bottom: conversion after maximally 200 h.

Table 2. Recycling of immobilized catalysts: maximal conversion of **22** [%], (ratio **23**:**24**), and [ratio of dimer, linear trimers, and linear tetramers] for every run with the amount of **24** set to 1 as the standard; TON gives the number of alkyne molecules converted by each metal center after 12 runs.

Cycle	Catalyst						
	16i	**17i**	**18i**	**19i**	**10i**	**12i**	**14i**
1	100 (4.80) [0.6, 0.5, 0.85]	93.1 (2.56) [0.06, –, 0.05]	100 (5.18) [0.46, 0.66, 1.02]	100 (4.90) [0.4, 0.56, 0.95]	100 (5.62) [0.87, 0.51, 0.71]	100 (4.83) [0.77, 0.53, 1.01]	100 (3.66) [0.42, 0.2, 0.52]
2	95.9 (2.28) [0.14, –, 0.12]	94.6 (1.80) [–, –, –]	98.8 (3.26) [0.26, –, 0.36]	100 (3.84) [0.34, 0.24, 0.48]	95.9 (2.78) [0.61, –, 0.15]	95.1 (3.47) [0.16, –, 0.29]	91.3 (1.96) [0.04, –, 0.06]
3	89.1 (1.61) [–, –, 0.03]	77.9 (0.78) [0.06, –, –]	93.1 (1.44) [–, –, 0.05]	90.5 (1.76) [0.05, –, 0.04]	87.1 (1.98) [0.03, –, –]	83.4 (1.80) [–, –, –]	71.4 (1.07) [0.09, –, –]
4	84.3 (1.09) [0.08,–,–]	81.7 (0.85) [0.08,–,–]	88.6 (1.11) [–, –, –,]	67.8 (1.04) [–, –, –]	71.8 (1.53) [0.10, –, –]	69.5 (1.34) [–, –, 0.07]	61.3 (0.86) [0.11, –, –]
5	70.0 (0.69) [0.12, –, –]	61.1 (0.94) [–, –, –]	80.2 (0.99) [–, –, –,]	61.8 (1.01) [0.06, –, –]	63.9 (1.32) [0.11, –, –]	57.4 (0.95) [0.12, –, 0.05]	65.5 (0.93) [0.17, –, –]
6	60.6 (0.80) [0.18, –, –]	38.3 (0.88) [0.19, –, –]	69.0 (0.90) [–, –, –,]	54.6 (0.92) [0.11, –, –]	62.2 (1.0) [0.10, –, –]	52.3 (0.87) [0.13, –, –]	77.2 (1.11) [0.10, –, –]
7	55.4 (0.88) [0.16, –, –]	42.6 (0.82) [0.19, –, –]	56.2 (0.75) [0.10, –, –,]	47.8 (1.0) [0.08, –, –]	40.3 (0.81) [0.22, –, –]	48.8 (0.85) [0.13, –, –]	58.4 (0.98) [0.10, –, –]
8	41.7 (0.92) [0.25, –, –]	68.8 (0.89) [0.15, –, –]	52.4 (0.94) [0.13, –, –]	36.0 (0.84) [0.22, –, –]	63.9 (0.78) [0.10, –, –]	37.4 (0.83) [0.18, –, –]	59.1 (0.93) [0.06, –, –]
9	34.0 (0.79) [0.26, –, –]	43.4 (0.89) [0.24, –, –]	48.6 (0.83) [0.17, –, –]	32.6 (0.85) [0.23, –, –]	58.1 (0.88) [0.14, –, –]	34.0 (0.85) [0.25, –, –]	68.6 (1.05) [0.07, –, –]
10	31.9 (0.85) [0.25, –, –]	61.7 (0.94) [0.23, –, –]	45.3 (0.84) [0.20, –, –]	33.2 (0.81) [0.21, –, –]	52.9 (0.84) [0.11, –, 0.06]	27.0 (0.86) [0.29, –, –]	49.8 (0.94) [0.08, –, –]
11	36.1 (0.86) [0.27, –, 0.07]	39.5 (0.91) [0.24, –, –]	35.0 (0.80) [0.28, –, –]	31.2 (0.86) [0.24, –, –]	44.3 (0.91) [0.17, –, –]	26.4 (0.81) [0.33, –, –]	53.7 (1.04) [0.10, –, –]
12	36.2 (0.84) [0.28, –, –]	38.1 (0.83) [0.17, –, –]	29.1 (0.83) [0.24, –, –]	26.1 (0.84) [0.23, –, –]	35.9 (0.83) [0.22, –, 0.07]	26.8 (0.86) [0.30, –, –]	36.1 (0.82) [0.20, –, –]
TON	1470	1481	1592	1363	1552	1317	1584

catalytic run. Furthermore, the supernatant solution does not have to be filtered prior to its application to the GC column, as it has to be done for runs with homogeneous catalysts. Thus, the work-up and analytics are much easier for the immobilized catalysts.

Recycling of the Immobilized Catalysts

The main advantage of the immobilized catalysts, however, is their potential for easy recycling. Here, the immobilized catalysts **10i**, **12i**, **14i**, and **16i – 19i** show their value: they can be subjected to 12 cycles with a final conversion of still between 30 and 40%. This is shown, for example, for **18i** in Figure 9. The maximal conversion of **22** after every run, and the ratio of 1,2,4-triphenylbenzene (**23**) to 1,3,5-triphenylbenzene (**24**) are given in Table 2 for the immobilized catalysts.

The maximal turnover numbers (TON) for all the catalysts after 12 runs (Table 2) are around 1500. The highest TON is achieved for **18i** with 1592 in 12 cycles, a value much higher than obtained previously. Although the differences in the product yields are not decisive enough to make far-reaching assumptions about the best ligand, those chelate ligands with C_3 bridges seem to be slightly superior to the ones with dppe-type bridges. No correlation of the linker length or type with the efficiency of the catalysts can be found. Regarding the monodentate phosphines, although the triarylphosphine ligand produces the most active catalyst in the first run, in the course of 12 cycles it deteriorates more quickly (overall TON only 1317) than the complexes with alkyldiarylphosphine or aryldialkylphosphine ligands.

As already indicated in preliminary communications, the maximal yields of products can be increased by a continuous design of the reactions,[12] because the catalytic systems are sensitive towards disturbances by cooling, opening and recharging the Schlenk flask. This is also proved by the ^{31}P CP/MAS spectra of the spent catalysts after 12 runs: besides the signal of the original catalyst, peaks of oxidic species are always and in some cases those of uncomplexed surface-bound phosphines are visible. The assumption that the system is disturbed by recharging the reaction vessel is further corroborated by the fact that one single addition of an excess of **22** to one batch of **18i** gives the high TON of 4810.

Another option that immobilized catalysts offer as compared to homogeneous ones is that the metal centers can be diluted on the support surface. In this way, deactivation by dimerization[73] has, for example, successfully been curbed back in the case of Wilkinson-type Rh hydrogenation catalysts.[14] Although in the case of carbonylnickel catalysts the main decomposition mechanism is the loss of the metal fragment from the phosphine linker, the surface dilution also seems to play a role.[12] For example, if **18i** is diluted to one fourth (about 4 metal centers per 100 nm^2) of the maximal surface density (16), a record TON of 7616 in one cycle with an excess of **22** can be obtained. With the usual recycling procedure (Table 2) **18i** with one fourth of the maximal surface coverage shows still a conversion of 88% in the 7th run. In contrast to this, one half of the maximal coverage with **18i** makes no difference as compared to **18i** with maximal density on the surface, the conversion in the 7th run is about 56%. This result shows that the metal centers need a minimum distance to each other, so that they are kept from forming dimers or oligomers. So, yet another deactivation mechanism for carbonylnickel phosphine catalysts seems to be an aggregation of the activated nickel centers. In the homogeneous phase this is obvious by the formation of a shiny layer of metallic nickel on the glass surface of the flask. The effect of surface dilution on the catalytic activity of the catalysts also corroborates the assumption that the molecules are evenly distributed over the surface after immobilization, and no patches are formed by cross-linking of the ethoxysilane groups or "self-assembly" of the linkers. It is also possible to improve the efficiency of immobilized catalysts with monodentate ligands. For example, in the case of **10i** half (5 molecules per 100 nm^2) of the maximal surface coverage already gives a decisive improvement: In the seventh run the conversion of **22** is still about 89%, while **10i** with maximal density is already down to about 40%. So, the effect of dilution of the catalyst on the surface is of a general nature, and independent of the ligands or metal centers.

Selectivity of the Catalysts

In homogeneous catalysis the main products with phenylacetylene (**22**) as the substrate are the unsymmetric and symmetric cyclotrimer **23** and **24**, linear trimers, and linear tetramers. Only traces of dimers are found. As shown in Table 3, the catalysts are overall more selective towards the formation of the unsymmetric cyclotrimer **23**, when the temperature is lower. For example, in the case of **17** the ratio of **23**:**24** increases from 2.4:1 to 7.5:1 when the temperature is lowered from 155 °C to 100 °C. However, the percentage of linear trimers and tetramers is greater at lower temperatures. For **17**, their ratio with respect to **24** (set to 1) is 0.6:0.7 at 155 °C, and 2.0:1.7 at 100 °C. Thus, one can use the temperature effect in order to drive the catalysis in the preferred direction. Another interesting feature is that the catalysts with monodentate ligands are more selective with respect to the formation of **23** than those with chelating ligands. For example, for **10** at 100 °C a ratio of **23** to **24** of 10.1:1 is obtained, and at 70 °C even of 14.1:1. The highest ratio obtained with the chelate complex **16** at 100 °C is only 7.6:1. While at 100 °C there is no difference in selectivity among the chelate complexes, at 155 °C those with the larger dppp-type bridge are more selective towards the formation of **23** than those with the dppe-type phosphine ligand. So, overall the homogeneous catalysts become more selective, the better they can assume tetrahedral ligand arrangement.

Table 3. Product ratio of 1,2,4-triphenylbenzene **23** to the dimer, linear trimers, and linear tetramers with respect to **24** (set to 1 as standard) at 100 °C, [155 °C], and (70 °C).

Product Ratio Catalyst	**23**	Linear Trimers	Linear Tetramers
10	10.1 (14.1)	2.0 (2.7)	1.4 (1.7)
12	8.1 (10.4)	1.7 (1.8)	1.0 (1.0)
13	5.3 [5.4]	1.3 [1.0]	1.0 [1.1]
14	7.0 [5.6]	1.7 [1.2]	1.4 [1.2]
16	7.6 [2.9]	2.3 [0.7]	1.3 [0.7]
17	7.5 [2.4]	2.0 [0.6]	1.7 [0.7]
18	7.1 [5.0]	1.5 [1.2]	1.4 [1.3]
19	6.9 [4.6]	1.7 [1.0]	1.3 [1.1]

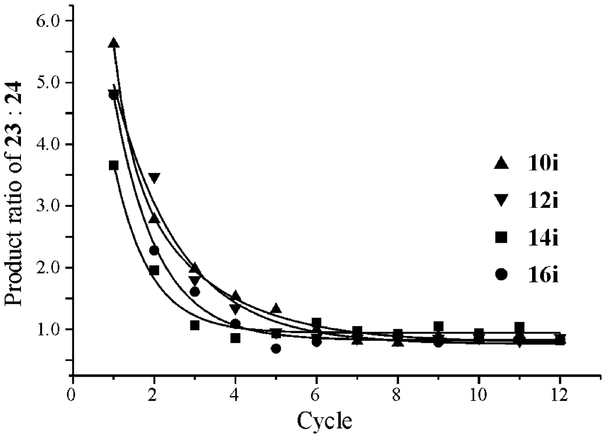

Figure 10. Product ratio of 1,2,4- to 1,3,5-triphenylbenzene **23**:**24** for the catalysts **10i**, **12i**, **14i**, and **16i** in the course of 12 cycles.

As can be seen in Table 2, in the case of the immobilized catalysts the amount of linear products is reduced substantially in all runs. Generally, after the fifth run, there are no more trimers or tetramers to be found, and only traces of the dimer. Interestingly, in the course of the recycling experiments, and also during one single run, the product ratio of **23** to **24** gradually becomes smaller, and finally reaches a plateau value of about 1:1 for every catalyst. This can be seen in Figure 10 for a variety of immobilized catalysts with mono- and bidentate phosphine linkers.

The same result is found in the case of **10i**, operated in a pseudo-continuous manner.[12] Therefore, we deduce that the selectivity of immobilized catalysts is not governed by the bite angle or spacer length of the linker phosphine. The change also does not correlate with the loss of catalytic activity, or the decomposition of the catalyst, as seen by solid-state NMR. The catalysts must change in a common, general way. The elucidation of this process will be the subject of future investigations with still more elaborate analytical tools.

Conclusion

In this work we have synthesized and characterized a variety of new carbonylnickel catalysts, and we have immobilized them cleanly on silica by mono- or bidentate phosphine linkers. The success of the immobilization has been shown by ^{31}P solid-state NMR, as well as the fate of the catalysts during catalysis. The temperature and solvent play major roles for the cyclotrimerizations. The immobilized catalysts can be recycled many times, and record turnover numbers are achieved. The selectivities can be tuned with the choice of temperature and phosphine bite angle in the case of homogeneous catalysts, and with reaction time for immobilized species. The activities of the immobilized catalysts can be further enhanced by continuous catalysis and diluting the metal centers on the surface.

Experimental Section

General Remarks

All reactions were performed by standard Schlenk techniques or in a glove-box in an oxygen-free nitrogen atmosphere. The solvents were dried by boiling over Na (cyclooctane over $\mathrm{CaH_2}$) and distilled and kept under nitrogen. The NMR spectra were recorded on Bruker instruments at the indicated magnetic fields. The solid-state NMR measurements were done with an Avance 400 wide-bore machine equipped with a 4 mm MAS probehead. For details of the solid-state NMR parameters see ref.[19]

Syntheses of Phosphines 1 to 5

The compounds **1–3**,[9,17] and **4**, **5**[10] have been synthesized and characterized as described previously.

Synthesis of Phosphines 6 to 9

Compounds **6** to **9** were synthesized by irradiating $\mathrm{Ph_2P(CH_2)_2PPhH}$[74] or $\mathrm{Ph_2P(CH_2)_3PPhH}$[74] in the presence of 1.2 equivalents of commercially available vinyl- or allyltriethoxysilane with UV light in a standard quartz apparatus with stirring and water cooling. The surplus of starting silane was then removed by Kugelrohr distillation at 120 °C under reduced pressure (0.02 mbar). Typical yields of the viscous oils were 89% (**6**), 92% (**7**), 93% (**8**), and 91% (**9**). Compound **6** has been described previously.[10]

Phosphine 7: ^{1}H NMR (300.1 MHz, $\mathrm{C_6D_6}$): $\delta = 7.45–7.38$ (m, H_o, PPh, 2H), 7.38–7.29 (m, H_o, $\mathrm{PPh_2}$, 4H), 7.10–7.05 (m, $\mathrm{H}_{m,\,p}$, PPh, 3H), 7.05–6.95 (m, $\mathrm{H}_{m,\,p}$, $\mathrm{PPh_2}$, 6H), 3.73 (q, $\mathrm{OCH_2}$, $^3J_{\mathrm{H,H}} = 7.0$ Hz, 6H), 2.25–2.04 (m, $\mathrm{Ph_2PC\underline{H}_2}$, 2H), 1.90–1.76 (m, $\mathrm{C\underline{H}_2CH_2Si}$, 2H), 1.73–1.60 (m, $\mathrm{PhPC\underline{H}_2}$, 4H), 1.11 (t, $\mathrm{CH_3}$, $^3J_{\mathrm{H,H}} = 7.0$ Hz, 9H), 0.85–0.76 (m, $\mathrm{CH_2Si}$, 2H); ^{13}C NMR (75.5 MHz, $\mathrm{C_6D_6}$): $\delta = 139.4$, 139.2 (d, C_i, $\mathrm{PPh_2}$, $^1J_{\mathrm{P,C}} = 15.2$ Hz), 139.1 (d, C_i, PPh, $^1J_{\mathrm{P,C}} = 17.3$ Hz), 133.2, 133.0 (d, C_o, $\mathrm{PPh_2}$, $^2J_{\mathrm{P,C}} = 18.0$ Hz), 132.9 (d, C_o, PPh, $^2J_{\mathrm{P,C}} = 19.4$ Hz), 128.7 (d, C_m, $^3J_{\mathrm{P,C}} = 5.5$ Hz), 128.9, 128.6 (s, C_p, $\mathrm{PPh_2}$), 128.6 (d, $\mathrm{C_p}$, PPh, $^4J_{\mathrm{P,C}} = 1.4$ Hz), 58.4 (s, $\mathrm{OCH_2}$), 32.0 (d, $\mathrm{\underline{C}H_2CH_2CH_2Si}$, $^1J_{\mathrm{P,C}} = 13.1$ Hz), 24.7 (pseudo-t, $\mathrm{Ph_2P\underline{C}H_2}$, $^1J_{\mathrm{P,C}} = {}^2J_{\mathrm{P,C}} = 15.3$ Hz), 24.6 (pseudo-t, $\mathrm{PhP\underline{C}H_2}$, $^1J_{\mathrm{P,C}} = {}^2J_{\mathrm{P,C}} = 14.5$ Hz), 20.1 (d, $\mathrm{\underline{C}H_2CH_2Si}$, $^2J_{\mathrm{P,C}} = 15.9$ Hz), 18.6 (s, $\mathrm{CH_3}$), 12.9 (d, $\mathrm{\underline{C}H_2Si}$, $^3J_{\mathrm{P,C}} = 11.1$ Hz); ^{31}P NMR (121.5 MHz, THF): $\delta = -12.7$ (d, $\mathrm{\underline{P}Ph_2}$, $^3J_{\mathrm{P,P}} = 26.8$ Hz), -21.6 (d, $\mathrm{\underline{P}Ph}$, $^3J_{\mathrm{P,P}} = 26.8$ Hz); anal. calcd. for $\mathrm{C_{29}H_{40}O_3P_2Si}$ (526.67): C 66.14, H 7.66, P 11.76; found: C 66.33, H 7.40, P 11.25.

Phosphine 8: ^{1}H NMR (300.1 MHz, $\mathrm{C_6D_6}$): $\delta = 7.52–7.44$ (m, H_o, PPh, 2H), 7.43–7.33 (m, H_o, $\mathrm{PPh_2}$, 4H), 7.13–7.00 (m, $\mathrm{H}_{m,\,p}$, 9H), 3.73 (q, $\mathrm{OCH_2}$, $^3J_{\mathrm{H,H}} = 7.0$ Hz, 6H), 2.34–2.28 (m, $\mathrm{Ph_2PC\underline{H}_2}$, 2H), 2.05–1.92 (m, $\mathrm{C\underline{H}_2CH_2Si}$, 2H), 1.90–1.83 (m, $\mathrm{PhPC\underline{H}_2}$, 2H), 1.73–1.68 (m, $\mathrm{Ph_2PCH_2C\underline{H}_2}$, 2H), 1.12 (t, $\mathrm{CH_3}$, $^3J_{\mathrm{H,H}} = 7.0$ Hz, 9H), 0.90–0.69 (m, $\mathrm{CH_2Si}$, 2H); ^{13}C NMR (75.5 MHz, $\mathrm{C_6D_6}$): $\delta = 139.8$ (d, C_i, $\mathrm{PPh_2}$, $^1J_{\mathrm{P,C}} = 15.2$ Hz), 139.7 (d, C_i, $\mathrm{PPh_2}$, $^1J_{\mathrm{P,C}} = 14.5$ Hz), 139.4 (d, C_i, PPh, $^1J_{\mathrm{P,C}} = 18.0$ Hz), 133.2, 133.1, 132.9 (d, C_o, $^2J_{\mathrm{P,C}} = 18.7$ Hz), 128.6 (d, C_m, $\mathrm{PPh_2}$, $^3J_{\mathrm{P,C}} = 6.9$ Hz) 128.5 (d, C_m, PPh, $^3J_{\mathrm{P,C}} = 6.9$ Hz), 128.8, 128.6, 128.6 (s, C_p), 58.5 (s, $\mathrm{OCH_2}$), 30.1 (dd, $\mathrm{Ph_2P\underline{C}H_2}$, $^1J_{\mathrm{P,C}} = 13.1$ Hz, $^3J_{\mathrm{P,C}} = 11.1$ Hz), 29.8 (dd, $\mathrm{PhP\underline{C}H_2}$, $^1J_{\mathrm{P,C}} = 14.5$ Hz, $^3J_{\mathrm{P,C}} = 12.5$ Hz), 22.9 (dd, $\mathrm{Ph_2PCH_2\underline{C}H_2}$, $^2J_{\mathrm{P,C}} = 15.2$ Hz, $^2J_{\mathrm{P,C}} = 17.3$ Hz), 21.4 (d, $\mathrm{\underline{C}H_2CH_2Si}$, $^1J_{\mathrm{P,C}} = 14.5$ Hz), 18.5 (s, $\mathrm{CH_3}$), 6.7 (d, $\mathrm{\underline{C}H_2Si}$, $^2J_{\mathrm{P,C}} = 10.4$ Hz); ^{31}P NMR (121.5 MHz, $\mathrm{C_6D_6}$): $\delta = -17.2$ (s, $\mathrm{\underline{P}Ph_2}$), -18.8 (s, $\mathrm{\underline{P}Ph}$); anal. calcd. for $\mathrm{C_{29}H_{40}O_3P_2Si}$ (526.67): C 66.14, H 7.66, P 11.76, found: C 66.20, H 7.41, P 11.21.

Phosphine 9: ^{1}H NMR (300.1 MHz, $\mathrm{C_6D_6}$): $\delta = 7.45–7.39$ (m, H_o, PPh, 2H), 7.38–7.28 (m, H_o, $\mathrm{PPh_2}$, 4H), 7.08–6.92 (m, $\mathrm{H}_{m,\,p}$, 9H), 3.71 (q, $\mathrm{OCH_2}$, $^3J_{\mathrm{H,H}} = 7.0$ Hz, 6H), 2.06–1.92 (m, $\mathrm{Ph_2PC\underline{H}_2}$, 2H), 1.75–1.50 (m, $\mathrm{PhP\underline{C}H_2}$, $\mathrm{C\underline{H}_2CH_2CH_2Si}$, $\mathrm{CH_2C\underline{H}_2CH_2Si}$, $\mathrm{Ph_2PCH_2C\underline{H}_2}$, 8H), 1.08 (t, $\mathrm{CH_3}$, $^3J_{\mathrm{H,H}} = 7.0$ Hz, 9H), 0.86–0.71 (m, $\mathrm{CH_2Si}$, 2H); ^{13}C NMR (75.5 MHz, $\mathrm{C_6D_6}$): $\delta = 140.1$, 139.9 (d, $\mathrm{PPh_2}$, C_i, $^1J_{\mathrm{P,C}} = 13.1$ Hz), 140.0 (d, C_i, PPh, $^1J_{\mathrm{P,C}} = 15.2$ Hz), 133.4 (d, C_o, PPh, $^2J_{\mathrm{P,C}} = 18.7$ Hz), 133.4. 133.3, (d, C_o, $\mathrm{PPh_2}$, $^2J_{\mathrm{P,C}} = 18.8$ Hz), 129.1 (d, C_m, PPh, $^3J_{\mathrm{P,C}} = 5.7$ Hz), 129.1, 129.0 (d, C_m, $\mathrm{PPh_2}$, $^3J_{\mathrm{P,C}} = 6.6$ Hz), 129.2, 128.8, 128.8 (s, C_p), 58.9 (s, $\mathrm{OCH_2}$), 32.7 (d, $\mathrm{\underline{C}H_2CH_2CH_2Si}$, $^1J_{\mathrm{P,C}} = 13.2$ Hz), 30.8 (pseudo-t, $\mathrm{Ph_2P\underline{C}H_2}$, $^1J_{\mathrm{P,C}} = {}^3J_{\mathrm{P,C}} = 13.2$ Hz), 30.6 (dd, $\mathrm{PhP\underline{C}H_2}$, $^1J_{\mathrm{P,C}} = 13.2$ Hz, $^3J_{\mathrm{P,C}} = 11.3$ Hz), 23.4 (pseudo-t, $\mathrm{Ph_2PCH_2\underline{C}H_2}$, $^2J_{\mathrm{P,C}} = {}^2J_{\mathrm{P,C}} = 16.5$ Hz), 20.7 (d, $\mathrm{\underline{C}H_2CH_2Si}$, $^2J_{\mathrm{P,C}} = 16.0$ Hz), 19.1 (s, $\mathrm{CH_3}$), 13.4 (d, $\mathrm{\underline{C}H_2Si}$, $^3J_{\mathrm{P,C}} = 11.3$ Hz); ^{31}P NMR (121.5 MHz, $\mathrm{C_6D_6}$): $\delta = -17.5$ (s, $\mathrm{\underline{P}Ph_2}$), -27.7 (s, $\mathrm{\underline{P}Ph}$); anal. calcd. for $\mathrm{C_{30}H_{42}O_3P_2Si}$ (540.69): C 66.64, H 7.83, P 11.46; found: C 67.04, H 7.86, P 11.33.

Synthesis of the Nickel Complexes 10 – 19

The syntheses and characterization of the compounds **10**,[9] **12**,[9] and **16**[10] have been described in the indicated references.

Compound 11: To 1.46 g (2 mmol) $[HO(CH_2)_4PPh_2]_2NiCl_2$ (synthesis analogous to the one described below for **15**) in 10 mL THF was added 0.19 g (3 mmol, 1.5 equiv.) of Zn powder in a stream of CO. The mixture turned pale yellow during 1 h of stirring at ambient temperature. After removal of the excess Zn by filtration and removal of the solvent under vacuum, the residue was recrystallized at 80 °C from $EtOH/H_2O$ (1:1). After further recrystallization from EtOH/hexane a slightly yellow crystalline product was obtained; yield: 0.29 g (24%, 0.46 mmol). Data from the crystal structure see Figure 3 and ref.[65] IR (KBr): $\nu = 3371$ (OH) 1991 (CO), 1935 cm^{-1} (CO); ^1H NMR (300.1 MHz, acetone-d_6): $\delta = 7.42 - 7.33$ (m. H_{aryl}, 2OH), 3.35 (t, CH_2OH, $^3J_{H,H} = 6.7$ Hz, 4H), 1.83 (dt, PCH_2, $^2J_{P,H} = 9.8$ Hz, $^3J_{H,H} = 6.7$ Hz, 4H), 1.33 (q, $C\underline{H}_2CH_2OH$, $^3J_{H,H} = 6.7$ Hz, 4H), 1.21 (m, $PCH_2C\underline{H}_2$, 4H); ^{13}C NMR (75.5 MHz, THF-d_8): $\delta = 201.2$ (t, $\underline{C}O$, $^2J_{P,C} = 2.2$ Hz), 139.7 (dd, C_i, $^1J_{P,C} = 18.2$ Hz. $^3J_{P,C} = 14.7$ Hz), 132.9 (t, C_o, $^2J_{P,C} = {}^4J_{P,C} = 6.6$ Hz), 129.3 (s, C_p), 128.6 (t, C_m, $^3J_{P,C} = {}^5J_{P,C} = 4.4$ Hz), 61.9 (s, CH_2OH), 35.3 (t, PCH_2, $^1J_{P,C} = {}^3J_{P,C} = 7.2$ Hz), 30.7 (dd, $PCH_2\underline{C}H_2$, $^2J_{P,C} = 12.2$ Hz, $^4J_{P,C} = 10.0$ Hz), 21.5 (t, $\underline{C}H_2CH_2OH$, $^3J_{P,C} = {}^5J_{P,C} = 3.9$ Hz); ^{31}P NMR (121.5 MHz, acetone-d_6): $\delta = 25.2$; anal. calcd. for $C_{34}H_{38}NiO_4P_2$ (631.304 g/mol): C 64.69, H 6.07, P 9.81; found: C 64.19, H 6.12, P 9.66.

Compound 13: To a suspension of 2.69 g (4.82 mmol) of **15** in 40 mL EtOH 0.47 g of Zn powder were added in a stream of CO. After 1.5 h of stirring at ambient temperature the bubbling in of CO was stopped. After filtration and removal of the solvent under vacuum a light brown oil remained. Recrystallization with $EtOH/H_2O$ gave **13** as slightly yellow crystals; yield: 1.56 g (2.85 mmol, 59.5%). Data from the crystal structure, see Figure 2 and ref.[64] IR (KBr): $\nu = 2000$ (CO), 1937 cm^{-1} (CO); ^1H NMR (300.1 MHz, acetone-d_6): $\delta = 7.23 -$ 7.77 (m, H_{aryl}, 20H), 4.43 (d, $O\underline{H}$, $^3J_{H,H} = 5$ Hz), 3.61 (m, CH), 3.13 (dd, CH_2, $^2J_{H,H} = 13.2$ Hz, $^3J_{H,H} = 11.7$ Hz, 2H), 2.15 (dd, CH_2, $^2J_{H,H} = 13.2$ Hz, $^3J_{H,H} = 12.8$ Hz, 2H); ^{13}C NMR (125.8 MHz, acetone-d_6): $\delta = 199.0$ (t, $\underline{C}O$, $^2J_{P,C} = 3.4$ Hz), 139.0 (dd, C_i, $^1J_{P,C} = 23.3$ Hz, $^3J_{P,C} = 20.8$ Hz), 136.6 (dd, $C_{i'}$, $^1J_{P,C} = 15.7$ Hz, $^3J_{P,C} = 12.3$ Hz), 132.1 (pseudo-t, C_o, $^2J_{P,C} = {}^4J_{P,C} = 7.2$ Hz), 131.3 (pseudo-t, $C_{o'}$, $^2J_{P,C} = {}^4J_{P,C} = 8.1$ Hz), 129.4 (s, C_p), 129.2 (s, $C_{p'}$), 128.4 (pseudo-t, C_m, $^3J_{P,C} = {}^5J_{P,C} = 4.7$ Hz), 128.2 (pseudo-t, $C_{m'}$, $^3J_{P,C} = {}^5J_{P,C} = 4.7$ Hz), 65.0 (t, $\underline{C}HOH$, $^2J_{P,C} = 16.5$ Hz), 38.6 (dd, CH'_2, $^1J_{P,C} = 11.4$ Hz, $^3J_{P,C} = 8.3$ Hz); ^{31}P NMR (121.5 MHz, THF): $\delta = 18.4$ (s); HRMS (FAB): calcd. for $C_{27}H_{26}NiO_3P_2$ [M – 2CO]: 486.0821, 488.0777; found: 486.0812 (100), 488.0778 (42.9).

Compound 14: A solution of 259 mg (0.94 mmol) of $(COD)_2Ni$ in 30 mL of toluene was cooled to – 30 °C. Then, a solution of 554 mg (0.94 mmol) of **5**[10] in 5 mL of toluene was added dropwise. The yellow reaction mixture turned dark red immediately. The mixture was stirred for 0.5 h at – 30 °C. Then CO was bubbled through the sample for 2 h at – 30 °C. The mixture was warmed to room temperature and became yellow. Removal of the solvent and flash chromatography on reversed phase silica gave **14** as a slightly yellow oil; yield: 530 mg (0.75 mmol, 80%); IR (KBr): $\nu = 1998$ (CO), 1933 cm^{-1} (CO); ^1H NMR (300.1 MHz, C_6D_6): $\delta = 7.83 - 7.59$ (m, H_o, 8H), 7.12 – 6.84 (m, $H_{m,p}$, 12H), 4.01 – 3.84 (m, CH), 3.70 (q, OCH_2, $^3J_{H,H} = 7.0$ Hz, 6H), 3.57 – 3.39 (m, CH_2, 2H), 2.26 – 2.06 (m, CH_2, 2H), 1.06 (t, CH_3, $^3J_{H,H} = 7.0$ Hz, 9H); ^{13}C NMR (125.8 MHz, C_6D_6): $\delta = 201.7$ (t, $\underline{C}O$, $^2J_{P,C} = 1.2$ Hz), 139.2 (pseudo-t, C_i, $^1J_{P,C} = {}^3J_{P,C} = 22.3$ Hz), 137.6 (dd, $C_{i'}$, $^1J_{P,C} = 15.0$ Hz, $^3J_{P,C} = 13.3$ Hz), 132.6 (d, C_o, $^2J_{P,C} = 7.3$ Hz), 132.0 (d, $C_{o'}$, $^2J_{P,C} = 7.9$ Hz), 129.4 (s, C_p), 129.3 (s, $C_{p'}$), 128.7 (d, C_m, $^3J_{P,C} = 4.8$ Hz), 128.5 (d, $C_{m'}$, $^3J_{P,C} = 4.8$ Hz), 68.1 (s, CHOSi), 59.4 (s, OCH_2), 39.8 (pseudo-t, CH_2, $^1J_{P,C} = {}^3J_{P,C} = 9.9$ Hz), 18.3 (s, CH_3); ^{31}P NMR (121.5 MHz, THF): $\delta = 18.4$ (s); HRMS (FAB): calcd. for $C_{33}H_{40}NiO_4P_2Si$ [M – 2 CO]: 648.1536, 650.1516; found: 648.1525 (100), 650.1479 (51.1); anal. calcd. for $C_{35}H_{40}NiO_6P_2Si$ (705.42): C 59.59, H 5.72, P 8.78; found: C 59.55, H 6.06, P 8.44.

Compound 15: To a solution of 0.86 g (3.6 mmol) of $NiCl_2 \cdot 6\,H_2O$ in EtOH a solution of 1.56 g (3.6 mmol) of **4** in THF was added. After 1 h of stirring, the dark red precipitate was filtered off and washed with EtOH whereby dark red crystals were obtained which were insoluble in the usual organic solvents; yield: 1.14 g (2.0 mmol, 56%). Therefore it was characterized by an X-ray analysis (Figure 1 and ref.[62]) and by solid-state NMR; ^{13}C CP/MAS NMR (TPPM decoupled,[19] 100.6 MHz, $\nu_{rot} = 15$ kHz): $\delta = 146.4 - 121.4$ (m, C_{aryl}), 65.2 (s, $\underline{C}H$), 39.7, 34.8 (s, CH_2); ^{31}P CP/MAS NMR (162.0 MHz, $\nu_{rot} = 13$ kHz): $\delta = 13.1, 6.9$; MS (FAB): $m/z = 521.1$ (M – Cl); anal. calcd. for $C_{27}H_{26}Cl_2NiOP_2$ (558.05): C 58.11, H 4.70, P 11.10; found: C 57.78, H 4.96, P 10.97.

Compound 17: A solution of 239 mg (0.45 mmol) of **7** in 5 mL of toluene was added in a dropwise manner to a solution of 125 mg (0.45 mmol) of $(COD)_2Ni$ in 30 mL of toluene, precooled to – 30 °C. The suspension turned dark red during 30 minutes of stirring at – 30 °C. During 2 h of bubbling in CO at – 30 °C, the color became lighter. Then the mixture was warmed to ambient temperature under prolonged admission of CO. After removal of the solvent and flash chromatography with reversed-phase silica, **17** was obtained as an orange oil; yield: 266 mg (0.41 mmol, 91.2%); IR (KBr): $\nu = 1995$ (CO), 1932 cm^{-1} (CO); ^1H NMR (300.1 MHz, C_6D_6): $\delta = 7.72$ (d, H_o, PPh, $^3J_{H,H} = 8.4$ Hz, 2H), 7.67 (d, H_o, PPh_2, $^3J_{H,H} = 9.0$ Hz, 2H), 7.52 (d, H_o, PPh_2, $^3J_{H,H} = 8.7$ Hz, 2H), 7.13 – 6.89 (m, $H_{m,p}$, 9H), 3.76 (q, OCH_2, $^3J_{H,H} = 6.9$ Hz, 6H), 2.03 – 1.53 (m, $Ph_2PC\underline{H}_2$, $\underline{C}H_2CH_2Si$, $PhPC\underline{H}_2$, $C\underline{H}_2CH_2CH_2Si$, 8H), 1.14 (t, CH_3, $^3J_{H,H} = 6.9$ Hz, 9H), 0.81 – 0.66 (m, CH_2Si, 2H); ^{13}C NMR (75.5 MHz, C_6D_6): $\delta = 202.9$ (d, $\underline{C}O$, $^2J_{P,C} = 3.5$ Hz), 202.7 (d, $\underline{C}O$, $^2J_{P,C} = 4.8$ Hz), 138.6 (dd, C_i, PPh_2, $^1J_{P,C} = 26.0$ Hz, $^3J_{P,C} = 5.2$ Hz), 138.4 (dd, C_i, PPh_2, $^1J_{P,C} = 25.6$ Hz, $^3J_{P,C} = 6.2$ Hz), 137.7 (dd, C_i, PPh, $^1J_{P,C} = 22.1$ Hz, $^3J_{P,C} = 5.5$ Hz), 133.2, 133.0, 132.8 (d, C_o, $^2J_{P,C} = 14.5$ Hz), 130.3 (d, C_p, PPh_2, $^4J_{P,C} = 1.4$ Hz), 130.1 (s, C_p, PPh), 129.8 (d, C_p, PPh_2, $^4J_{P,C} = 2.1$ Hz), 129.4, 129.3 (d, C_m, PPh_2, $^3J_{P,C} = 9.0$ Hz), 129.3 (d, C_m, PPh, $^3J_{P,C} = 9.7$ Hz), 59.0 (s, OCH_2), 35.7 (dd, $\underline{C}H_2CH_2CH_2Si$, $^1J_{P,C} = 15.6$ Hz, $^3J_{P,C} = 4.5$ Hz), 30.3 (dd, $Ph_2P\underline{C}H_2$, $^1J_{P,C} = 24.9$ Hz, $^2J_{P,C} = 21.5$ Hz), 28.9 (dd, $PhP\underline{C}H_2$, $^1J_{P,C} = 23.9$ Hz, $^2J_{P,C} = 22.5$ Hz), 20.0 (d, $\underline{C}H_2CH_2Si$, $^2J_{P,C} = 6.2$ Hz), 19.0 (s, CH_3), 13.4 (d, CH_2Si, $^3J_{P,C} = 13.1$ Hz); ^{31}P NMR (121.5 MHz, C_6D_6): $\delta = 46.6$ (d, PPh, $^3J_{P,P} = 35.9$ Hz), 42.2 (d, PPh_2, $^3J_{P,P} = 35.9$ Hz); HRMS (FAB): calcd. for $C_{29}H_{40}NiO_3P_2Si$ [M – 2 CO]: 584.1599, 586.1553; found: 584.1576 (100), 586.1530 (95.2); anal. calcd. for $C_{31}H_{40}NiO_5P_2Si$ (641.37): C 58.05, H 6.29, P 9.66; found: C 58.66, H 6.44, P 9.82.

Compound 18: The nickel complex **18** was synthesized according to the procedure given for **17**. IR (KBr): $\nu = 1992$ (CO), 1930 cm^{-1} (CO); ^1H NMR (300.1 MHz, C_6D_6): $\delta =$ 7.66 – 7.62 (m, H_o, PPh_2, 4H), 7.54 – 7.51 (m, H_o, PPh, 2H), 7.40 – 7.20 (m, $H_{m,p}$, 9H), 3.71 (q, OCH_2, $^3J_{H,H} = 6.7$ Hz, 6H), 2.34 – 2.28 (m, $Ph_2PC\underline{H}_2$, 2H), 2.05 – 1.92 (m, $\underline{C}H_2CH_2Si$, 2H), 1.90 – 1.83 (m, $PhPC\underline{H}_2$, 2H), 1.73 – 1.68 (m, $Ph_2PCH_2C\underline{H}_2$, 2H), 1.10 (t, CH_3, $^3J_{H,H} = 6.7$ Hz, 9H), 0.85 – 0.76 (m, CH_2Si, 2H); ^{13}C NMR (75.5 MHz, CD_2Cl_2): $\delta = 201.6$ (s, $\underline{C}O$), 138.7 (dd, C_i, PPh_2, $^1J_{P,C} = 27.3$ Hz, $^3J_{P,C} = 5.2$ Hz), 138.6 (dd, C_i, PPh_2, $^1J_{P,C} = 27.0$ Hz, $^3J_{P,C} = 6.2$ Hz), 136.5 (dd, C_i, PPh, $^1J_{P,C} = 24.2$ Hz, $^3J_{P,C} = 5.5$ Hz), 132.5, 132.4, 132.0 (d, C_o, $^2J_{P,C} = 13.8$ Hz), 129.8, 129.6, 129.3 (d, C_p, $^4J_{P,C} = 1.4$ Hz), 128.7, 128.5, 128.4 (d, C_m, $^3J_{P,C} = 9.0$ Hz), 58.6 (s, OCH_2), 29.7 (dd, $Ph_2P\underline{C}H_2$, $^1J_{P,C} =$ 21.1 Hz, $^3J_{P,C} = 2.4$ Hz), 29.2 (dd, $PhP\underline{C}H_2$, $^1J_{P,C} = 19.0$ Hz, $^3J_{P,C} = 2.4$ Hz), 25.7 (dd, $Ph_2PCH_2\underline{C}H_2$, $^2J_{P,C} = 15.9$ Hz, $^2J_{P,C} =$ 6.9 Hz), 19.8 (pseudo-t, $\underline{C}H_2CH_2Si$, $^1J_{P,C} = {}^3J_{P,C} = 3.8$ Hz), 18.4 (s, CH_3), 4.4 (s, CH_2Si); ^{31}P NMR (121.5 MHz, C_6D_6): $\delta = 17.1$ (s, PPh), 15.1 (s, PPh_2); HRMS (FAB): calcd. for $C_{29}H_{40}NiO_3P_{2\text{-}}$ 575 (100), 586.1530 (49.1); anal. calcd. for $C_{31}H_{40}NiO_5P_2Si$ (641.37): C 58.05, H 6.29; found: C 57.72, H 6.73.

Compound 19: The nickel complex **19** was synthesized according to the procedure given for **17**. IR (KBr): $\nu = 1992$ (CO), 1929 cm^{-1} (CO); ^{1}H NMR (500.1 MHz, C_6D_6): $\delta = 7.75$ (d, H_o, PPh, $^3J_{H,H} = 7.0$ Hz, 2H), 7.67 (d, H_o, PPh_2, $^3J_{H,H} =$ 6.7 Hz, 2H), 7.56 (d, H_o, PPh_2, $^3J_{H,H} = 7.0$ Hz, 2H), 7.14 – 6.89 (m, $H_{m,\,p}$, 9H), 3.79 (q, OCH_2, $^3J_{H,H} = 7.1$ Hz, 6H), 2.04 – 1.94 (m, $Ph_2PC\underline{H}_2$, 2H), 1.92 – 1.84 (m, $PhPC\underline{H}_2$, 2H), 1.79 – 1.39 (m, 6H, $\underline{C}H_2CH_2CH_2Si$, $\underline{C}H_2CH_2Si$, $Ph_2PCH_2C\underline{H}_2$), 1.17 (t, CH_3, $^3J_{H,H} = 7.1$ Hz, 9H), 0.80 – 0.68 (m, CH_2Si, 2H); ^{13}C NMR (125.8 MHz, C_6D_6): $\delta = 201.4$ (d, $\underline{C}O$, $^2J_{P,C} = 1.9$ Hz), 201.2 (d, $\underline{C}O$, $^2J_{P,C} = 3.8$ Hz), 138.7 (dd, C_i, PPh_2, $^1J_{P,C} = 26.9$ Hz, $^3J_{P,C} =$ 6.1 Hz)$^{\#}$, 138.4 (dd, C_i, PPh, $^1J_{P,C} = 26.8$ Hz, $^3J_{P,C} = 8.0$ Hz)$^{\#}$, 132.3, 132.1 (d, C_o, PPh_2, $^2J_{P,C} = 15.1$ H), 131.6 (d, C_o, PPh, $^2J_{P,C} = 14.1$ Hz), 129.1 (s, C_p, PPh_2), 128.6 (s, C_p, PPh), 128.2 (d, C_m, PPh_2, $^3J_{P,C} = 9.4$ Hz), 128.1 (d, C_m, PPh, $^3J_{P,C} = 9.4$ Hz), 58.1 (s, OCH_2), 35.8 (dd, $\underline{C}H_2CH_2CH_2Si$, $^1J_{P,C} = 17.0$ Hz, $^3J_{P,C} =$ 6.6 Hz), 29.3 (dd, $Ph_2P\underline{C}H_2$, $^1J_{P,C} = 20.3$ Hz, $^3J_{P,C} = 8.9$ Hz), 29.2 (dd, $PhP\underline{C}H_2$, $^1J_{P,C} = 20.1$ Hz, $^3J_{P,C} = 8.5$ Hz), 22.7 (br. s, $Ph_2PCH_2\underline{C}H_2$), 19.4 (pseudo-t, $\underline{C}H_2CH_2Si$, $^2J_{P,C} = {}^4J_{P,C} =$ 4.2 Hz), 18.2 (s, CH_3), 12.6 (d, CH_2Si, $^3J_{P,C} = 13.2$ Hz); ^{31}P NMR (121.5 MHz, C_6D_6): $\delta = 15.6$ (s, PPh), 10.0 (s, PPh_2); HRMS (FAB): calcd. for $C_{30}H_{42}NiO_3P_2Si$ [M – 2 CO]: 598.1705, 600.1625; found: 598.1732 (100), 600.1687 (49.7). $^{\#}$The signals of the *ipso*-C nuclei have only low intensity.

General Immobilization Procedure

All the molecular phosphines and nickel complexes were immobilized on Merck silica (specific surface area 750 m^2/g, average pore diameter 40 Å, particle size 70 to 230 mesh, predried at 600 °C under vacuum) by stirring an excess of the molecular compounds with a suspension of the support material in toluene at 60 °C for about 5 hours.[16–18] After decanting the supernatant solution, the silica was washed twice with toluene and twice with THF, and the surface coverages were determined by weighing back the molecular compounds after removing the solvents from the combined supernatant and washing solutions.[16–18] The surface coverages of all immobilized species were usually in the range of 12 to 19 molecules per 100 nm^2 of surface area. For suspension NMR[15] the THF slurries were used directly, for solid-state NMR the material was dried under vacuum at ambient temperature for at least 4 h. The solid-state NMR chemical shifts of the immobilized species were comparable to the ones of the molecules in solution (see Figure 4).

Homogeneous Catalysis

For all experiments with homogeneous catalysts, this standard procedure was applied, unless otherwise noted: X mg (usually 10 to 25 mg) of catalyst (0.5 mol % with respect to the substrate) in Y mL (usually 5 to 12 mL) of freshly distilled cyclooctane (0.5 mol/L substrate concentration) was heated to the reaction temperature in a 25-mL Schlenk flask. Then the catalysis was started by adding Z mL (usually 0.3 to 0.5 mL) of freshly distilled **22** *via* a syringe. Samples of 100 µL were taken at regular intervals from the reaction mixture, filtered through a small column of silica, and applied to the GC. The peak assignments in the chromatograms were made with standard samples of the pure compounds **23** and **24**, as well as with GC-MS for the linear oligomers. Every catalytic run was done twice, and the average value was used for the Figures and Tables presented here.

Catalysis with Immobilized Catalysts

X g of modified silica (depending on the surface coverage 80 to 160 mg, corresponding to about 7 to 20 mg of surface-bound catalyst) was placed into a 25-mL Schlenk flask. The silica was then suspended in Y mL (5 to 15 mL) of cyclooctane and heated to the reaction temperature with stirring. Then, the catalysis was started by addition of Z mL (0.25 to 0.6 mL) of freshly distilled **22**. Samples of 100 µL of the supernatant solution were taken at regular intervals from the reaction mixture, filtered through a small column of silica, and applied to the GC. For peak assignments see above. The maximal reaction time for one cycle was 8 days. After catalysis the reaction mixture was cooled, and the supernatant solution decanted. The solid catalyst was washed by stirring with 5 mL of heptane, and dried under vacuum for about 30 min after decanting all liquids. Then, the catalyst was either subjected to solid-state NMR analysis, or used for the next cycle. Every catalytic run was done twice, and the medium value was used for the Figures and Tables presented here.

Acknowledgements

We thank the Deutsche Forschungsgemeinschaft (SFB 623), and the Fonds der Chemischen Industrie (FCI) for financial support. We are also grateful for the help of Mrs. D. Rambow for preparing countless samples and supervising the catalytic runs.

References and Notes

[1] J. A. Gladysz, *Pure Appl. Chem.* **2001**, *73*, 1319.
[2] B. Cornils, W. A. Herrmann, *Applied Homogeneous Catalysis with Organometallic Compounds*, VCH, New York, **1996**.
[3] H. Gao, R. J. Angelici, *Organometallics* **1999**, *18*, 989.
[4] M. Wende, R. Meier, J. A. Gladysz, *J. Am. Chem. Soc.* **2001**, *123*, 11490, and literature cited therein.
[5] R. Akiyama, S. Kobayashi, *Angew. Chem.* **2001**, *113*, 3577.

[6] D. de Groot, B. F. M. de Waal, J. N. H. Reek, A. P. H. J. Schenning, P. C. J. Kamer, E. W. Meijer, P. W. N. M. van Leeuwen, *J. Am. Chem. Soc.* **2001**, *123*, 8453.

[7] F. R. Hartley, *Supported Metal Complexes*, D. Reidel Publishing Co, Dordrecht, Holland, **1985**.

[8] J. H. Clark, *Supported Reagents in Organic Reactions*, VCH, Weinheim, **1994**.

[9] K. D. Behringer, J. Blümel, *Inorg. Chem.* **1996**, *35*, 1814.

[10] G. Tsiavaliaris, S. Haubrich, C. Merckle, J. Blümel, *Synlett* **2001**, 391.

[11] K. D. Behringer, J. Blümel, *Chem. Commun.* **1996**, 653.

[12] S. Reinhard, K. D. Behringer, J. Blümel, *New J. Chem.*, in press.

[13] C. Merckle, S. Haubrich, J. Blümel, *J. Organomet. Chem.* **2001**, *627*, 44.

[14] C. Merckle, J. Blümel, *Adv. Synth. Catal.* **2003**, *345*, 584.

[15] C. Merckle, J. Blümel, *Chem. Mater.* **2001**, *13*, 3617.

[16] K. D. Behringer, J. Blümel, *J. Liquid Chromatogr.* **1996**, *19*, 2753.

[17] J. Blümel, *Inorg. Chem.* **1994**, *33*, 5050.

[18] J. Blümel, *J. Am. Chem. Soc.* **1995**, *117*, 2112.

[19] S. Reinhard, J. Blümel, *Magn. Reson. Chem.* **2003**, *41*, in press.

[20] K. D. Behringer, J. Blümel, *Z. Naturforsch.* **1995**, *50b*, 1723.

[21] Reviews on cyclotrimerization: S. Saito, Y. Yamamoto, *Chem. Rev.* **2000**, *100*, 2901; H.-W. Frühauf, *Chem. Rev.* **1997**, *97*, 523; M. Lautens, W. Klute, W. Tam, *Chem. Rev.* **1996**, *96*, 49; G. G. Melikyan, K. M. Nicholas, in *Modern Acetylene Chemistry*, (Eds.: P. J. Stang, F. Diederich), VCH, Weinheim, **1995**, pp. 99–138; D. B. Grotjahn, in *Comprehensive Organometallic Chemistry II*, (Eds.: E. W. Abel, F. G. A. Stone, G. Wilkinson), (Vol. Ed.: L. S. Hegedus), Pergamon, Oxford, **1995**, Vol. 12, pp. 741–770.

[22] S. A. Macgregor, E. Wenger, *Organometallics* **2002**, *21*, 1278.

[23] R. Herges, A. Papafilippopoulos, *Angew. Chem.* **2001**, *113*, 4809.

[24] K.-R. Pörschke, *J. Am. Chem. Soc.* **1989**, *111*, 5691.

[25] D. Peña, D. Pérez, E. Guitián, L. Castedo, *J. Org. Chem.* **2000**, *65*, 6944 and literature cited therein.

[26] C. Müller, R. J. Lachicotte, W. D. Jones, *Organometallics* **2002**, *21*, 1118 and 1975.

[27] M. A. Bennett, C. J. Cobley, A. D. Rae, E. Wenger, A. C. Willis, *Organometallics* **2000**, *19*, 1522.

[28] K. Ferré, L. Toupet, V. Guerchais, *Organometallics* **2002**, *21*, 2578.

[29] H. Hoberg, W. Richter, *J. Organomet. Chem.* **1980**, *195*, 355.

[30] M. Shanmugasundaram, M.-S. Wu, C.-H. Cheng, *Org. Lett.* **2001**, *3*, 4233; A. Jeevanandam, R. P. Korivi, I. Huang, C.-H. Cheng, *Org. Lett.* **2002**, *4*, 807.

[31] J. Montgomery, *Acc. Chem. Res.* **2000**, *33*, 467, and literature cited therein.

[32] O. V. Ozerov, F. T. Lapido, B. O. Patrick, *J. Am. Chem. Soc.* **1999**, *121*, 7941; O. V. Ozerov, B. O. Patrick, F. T. Lapido, *J. Am. Chem. Soc.* **2000**, *122*, 6423.

[33] D. Suzuki, H. Urabe, F. Sato, *J. Am. Chem. Soc.* **2001**, *123*, 7925; R. Tanaka, Y. Nakano, D. Suzuki, H. Urabe, F. Sato, *J. Am. Chem. Soc.* **2002**, *124*, 9682; D. Suzuki, R. Tanaka, H. Urabe, F. Sato, *J. Am. Chem. Soc.* **2002**, *124*, 3518.

[34] T. Takahashi, F.-Y. Tsai, Y. Li, K. Nakajima, M. Kotora, *J. Am. Chem. Soc.* **1999**, *121*, 11093; T. Takahashi, Z. Xi, A. Yamazaki, Y. Liu, K. Nakajima, M. Kotora, *J. Am. Chem. Soc.* **1998**, *120*, 1672.

[35] Y. Kishimoto, P. Eckerle, T. Miyatake, M. Kainosho, A. Ono, T. Ikariya, R. Noyori, *J. Am. Chem. Soc.* **1999**, *121*, 12035.

[36] H. Yan, A. M. Beatty, T. P. Fehlner, *Organometallics* **2002**, *21*, 5029; H. Yan, A. M. Beatty, T. P. Fehlner, *Angew. Chem.* **2001**, *113*, 4630.

[37] I. Ojima, A. T. Vu, J. V. McCullagh, A. Kinoshita, *J. Am. Chem. Soc.* **1999**, *121*, 3230.

[38] B. Witulski, T. Stengel, J. M. Fernández-Hernández, *Chem. Commun.* **2000**, 1965.

[39] Y. Yamamoto, R. Ogawa, K. Itoh, *Chem. Commun.* **2000**, 549.

[40] R. Ruan, J. Zhang, X. Zhou, R. Cai, *Chem. Commun.* **2002**, 538.

[41] A. Haskel, T. Straub, A. K. Dash, M. S. Eisen, *J. Am. Chem. Soc.* **1999**, *121*, 3014.

[42] R. Diercks, B. E. Eaton, S. Gürtzgen, S. Jalisatgi, A. J. Matzger, R. H. Radde, K. P. C. Vollhardt, *J. Am. Chem. Soc.* **1998**, *120*, 8247.

[43] L. Guo, J. D. Bradshaw, D. B. McConville, C. A. Tessier, W. J. Youngs, *Organometallics* **1997**, *16*, 1685.

[44] T. Nickel, R. Goddard, C. Krüger, K.-R. Pörschke, *Angew. Chem.* **1994**, *106*, 908.

[45] S. Saito, T. Kawasaki, N. Tsuboya, Y. Yamamoto, *J. Org. Chem.* **2001**, *66*, 796.

[46] N. Mori, S. Ikeda, K. Odashima, *Chem. Commun.* **2001**, 181.

[47] J. Li, H. Jiang, M. Chen, *J. Org. Chem.* **2001**, *66*, 3627.

[48] T. Sugihara, A. Wakabayashi, Y. Nagai, H. Takao, H. Imagawa, M. Nishizawa, *Chem. Commun.* **2002**, 576.

[49] N. Mori, S. Ikeda, Y. Sato, *J. Am. Chem. Soc.* **1999**, *121*, 2722.

[50] S. Han, D. R. Anderson, A. D. Bond, H. V. Chu, R. L. Disch, D. Holmes, J. M. Schulman, S. J. Teat, K. P. C. Vollhardt, G. D. Whitener, *Angew. Chem.* **2002**, *114*, 3361; S. Han, A. D. Bond, R. L. Disch, D. Holmes, J. M. Schulman, S. J. Teat, K. P. C. Vollhardt, G. D. Whitener, *Angew. Chem.* **2002**, *114*, 3357.

[51] S. Hecht, J. M. J. Fréchet, *J. Am. Chem. Soc.* **1999**, *121*, 4084.

[52] K. D. Behringer, J. Blümel, *Magn. Reson. Chem.* **1995**, *33*, 729.

[53] L. S. Meriwether, M. F. Leto, E. C. Colthup, G. W. Kennerly, *J. Org. Chem.* **1962**, *27*, 3930.

[54] K.-R. Pörschke, C. Pluta, B. Proft, F. Lutz, C. Krüger, *Z. Naturforsch.* **1993**, *48b*, 608.

[55] P. Giannoccaro, A. Sacco, G. Vasapollo, *Inorg. Chim. Acta* **1979**, *37*, L 455.

[56] K. Tanaka, Y. Kawata, T. Tanaka, *Chem. Lett.* **1974**, 831.

[57] J. Blümel, M. Herker, W. Hiller, F. H. Köhler, *Organometallics* **1996**, *15*, 3474; M. Schnellbach, F. H. Köhler, J. Blümel, *J. Organomet. Chem*. **1996**, *520*, 227.

[58] L. Bemi, H. C. Clark, J. A. Davies, C. A. Fyfe, R. E. Wasylishen, *J. Am. Chem. Soc*. **1982**, *104*, 438.

[59] P. S. Jarrett, P. J. Sadler, *Inorg. Chem*. **1991**, *30*, 2098.

[60] G. Booth, *Adv. Inorg. Chem. Radiochem*. **1964**, *6*, 1.

[61] J. Mason, *Multinuclear NMR*, Plenum Press, New York, **1987**.

[62] Red crystal (polyhedron), dimensions $0.28 \times 0.23 \times 0.19\ \mathrm{mm}^3$, crystal system monoclinic, space group $P2_1/c$, $Z = 4$, $a = 8.6869(4)$ Å, $b = 24.5197(11)$ Å, $c = 12.6866(6)$ Å, $\alpha = 90°$, $\beta = 109.101(1)°$, $\gamma = 90°$, $V = 2553.5(2)$ Å^3, ϱ=1.452 g/cm^3, T = 200(2) K, $2\Theta_{max}$=27.48°, radiation Mo-Kα, $\lambda = 0.71073$ Å, 0.3° ω-scans with CCD area detector, covering a whole sphere in reciprocal space, 26130 reflections measured, 5855 unique (R(int) = 0.0331), 4821 observed ($I > 2\sigma(I)$), intensities were corrected for Lorentz and polarization effects, an empirical absorption correction was applied using SADABS[66] based on the Laue symmetry of the reciprocal space, $\mu = 1.11\ \mathrm{mm}^{-1}$, T_{min} = 0.76, T_{max} = 0.83, structure solved by direct methods and refined against F^2 with a full-matrix least-squares algorithm using the SHELXTL-PLUS (5.10) software package,[67] 302 parameters refined, hydrogen atoms were treated using appropriate riding models except for H1, which was refined isotropically, goodness of fit 1.06 for observed reflections, final residual values R1(F) = 0.033, wR(F^2) = 0.077 for observed reflections, residual electron density –0.35 to 0.50 eÅ^{-3}. Further crystallographic data for this structure have been deposited with the Cambridge Crystallographic Data Center as supplementary publication no. CCDC 199727. These data can be obtained free of charge *via* www.ccdc.cam.ac.uk/conts/retrieving.html (or from the CCDC, 12 Union Road, Cambridge CB2 1EZ, UK; fax: +44 1223 336033; e-mail: deposit@ccdc.cam.ac.uk).

[63] S.-T. Liu, G.-J. Liu, C.-H. Yieh, M.-C. Cheng, S.-M. Peng, *J. Organomet. Chem*. **1990**, *387*, 83.

[64] Colorless crystal (polyhedron), dimensions $0.36 \times 0.21 \times 0.15\ \mathrm{mm}^3$, crystal system monoclinic, space group $P2_1/c$, $Z = 4$, $a = 8.3643(1)$ Å, $b = 31.4479(3)$ Å, $c = 10.4164(1)$ Å, $\alpha = 90°$, $\beta = 104.4210(10)°$, $\gamma = 90°$, $V = 2653.60(5)$ Å^3, ϱ=1.360 g/cm^3, T = 200(2) K, $2\Theta_{max}$=25.64°, radiation Mo-Kα, $\lambda = 0.71073$ Å, 0.3° ω-scans with CCD area detector, covering a whole sphere in reciprocal space, 19711 reflections measured, 4561 unique (R(int) = 0.0268), 3788 observed ($I > 2\sigma(I)$), intensities were corrected for Lorentz and polarization effects, an empirical absorption correction was applied using SADABS[66] based on the Laue symmetry of the reciprocal space, $\mu = 0.88\ \mathrm{mm}^{-1}$, T_{min} = 0.77, T_{max} = 0.90, structure solved by direct methods and refined against F^2 with a full-matrix least-squares algorithm using the SHELXTL-PLUS (5.10) software package,[67] 320 parameters refined, hydrogen atoms were treated using appropriate riding models except for H1, which was refined isotropically, goodness of fit 1.03 for observed reflections, final residual values R1(F) = 0.028, wR(F^2) = 0.064 for observed reflections, residual electron density –0.19 to 0.27 eÅ^{-3}. Further crystallographic data for this structure have been deposited with the Cambridge Crystallographic Data Center as supplementary publication no. CCDC 199726. These data can be obtained free of charge *via* www.ccdc.cam.ac.uk/conts/retrieving.html (or from the CCDC, 12 Union Road, Cambridge CB2 1EZ, UK; fax: +44 1223 336033; e-mail: deposit@ccdc.cam.ac.uk).

[65] Colorless crystal (polyhedron), dimensions $0.34 \times 0.16 \times 0.06\ \mathrm{mm}^3$, crystal system monoclinic, space group $P2_1/c$, $Z = 4$, $a = 19.4224(3)$ Å, $b = 10.0773(1)$ Å, $c = 17.6950(2)$ Å, $\alpha = 90°$, $\beta = 112.4390(10)°$, $\gamma = 90°$, $V = 3201.14(7)$ Å^3, ϱ=1.310 g/cm^3, T = 200(2) K, $2\Theta_{max}$ = 25.57°, radiation Mo-Kα, $\lambda = 0.71073$ Å, 0.3° ω-scans with CCD area detector, covering a whole sphere in reciprocal space, 23209 reflections measured, 5573 unique (R(int) = 0.0375), 4247 observed ($I > 2\sigma(I)$), intensities were corrected for Lorentz and polarization effects, an empirical absorption correction was applied using SADABS[66] based on the Laue symmetry of the reciprocal space, $\mu = 0.74\ \mathrm{mm}^{-1}$, T_{min} = 0.79, T_{max} = 0.96, structure solved by Patterson-method and refined against F^2 with a full-matrix least-squares algorithm using the SHELXTL-PLUS (5.10) software package,[67] 378 parameters refined, hydrogen atoms were treated using appropriate riding models except for H33 and H63 at the hydroxy groups, which were refined isotropically, goodness of fit 1.04 for observed reflections, final residual values R1(F) = 0.031, wR(F^2) = 0.064 for observed reflections, residual electron density –0.35 to 0.28 eÅ^{-3}. Further crystallographic data for this structure have been deposited with the Cambridge Crystallographic Data Center as supplementary publication no. CCDC 199728. These data can be obtained free of charge *via* www.ccdc.cam.ac.uk/conts/retrieving.html (or from the CCDC, 12 Union Road, Cambridge CB2 1EZ, UK; fax: +44 1223 336033; e-mail: deposit@ccdc.cam.ac.uk).

[66] Program SADABS V2.03 for absorption correction: G. M. Sheldrick, Bruker Analytical X-ray Division, Madison, Wisconsin, **2001**.

[67] Software package SHELXTL V5.10 for structure solution and refinement: G. M. Sheldrick, Bruker Analytical X-ray Division, Madison, Wisconsin, **1997**.

[68] C. Nachtigal, S. Al-Gharabli, K. Eichele, E. Lindner, H. A. Mayer, *Organometallics* **2002**, *21*, 105.

[69] M. Mizukami, M. Moteki, K. Kurihara, *J. Am. Chem. Soc*. **2002**, *124*, 12889.

[70] R. K. Iler, *The Chemistry of Silica*, John Wiley, New York, **1979**.

[71] D. R. Lide, in *C. R. C. Handbook of Chemistry and Physics*, 76th ed., C. R. C. Press, New York, **1995**.

[72] P. Dierkes, P. W. N. M. van Leeuwen, *J. Chem. Soc. Dalton Trans*. **1999**, 1519.

[73] U. Schubert, K. Rose, *Transition Met. Chem*. **1989**, *14*, 291.

[74] T.-S. Chou, C.-H. Tsao, S. C. Hung, *J. Organomet. Chem*. **1986**, *312*, 53.